A Chemical Kinetic Mechanism for Combustion and Flame Propagation of $CH_2F_2/O_2/N_2$ Mixtures

Donald R. Burgess, Jr.,[a] Valeri I. Babushok,[b] and Jeffrey A. Manion[a]

[a] Chemical Sciences Division, National Institute of Standards and Technology, Gaithersburg, MD 20899

[b] Energy and Environment Division, National Institute of Standards and Technology, Gaithersburg, MD 20899

Keywords: Hydrofluorocarbons; Flame propagation; Laminar burning velocity; Chemical kinetics; Reaction mechanism; Flame modeling

Submitted to Inter. J. Chem. Kinet. September 22, 2021

Final version for publication submitted December 2, 2021

Abstract

In this work, we compiled and evaluated rate expressions for reactions relevant to the decomposition and combustion of CH_2F_2 (difluoromethane, refrigerant R-32) in $CH_2F_2/O_2/N_2$ flames. The recommended values have been used in premixed flame calculations, reported elsewhere, to model experimentally-derived burning velocities determined using a constant volume spherical

flame method. In this work, we also provide a detailed description of the reaction pathways for decomposition and combustion of CH_2F_2. This work is part of a larger effort at NIST to characterize and predict the flammability of new refrigerant working fluids and their blends for consideration as replacements of current refrigerants with high global warming potentials (GWPs).

Introduction

Current refrigerants are generally halogenated and many have high global warming potentials (GWPs), a result of their long tropospheric lifetimes and high radiative efficiencies.[1-5] There are new refrigerants with lower GWPs, but their shorter tropospheric lifetimes (because of fewer halogens) comes at the expense of increased flammability (because of more hydrogens), which is a safety issue. Working fluids that best balance equipment needs, efficiency, safety, and GWP requirements may be mixtures, with each component having a different flammability. Optimization requires investigating the flammability behavior of a daunting variety of possible formulations over the wide range of fuel loadings and humidity conditions that may be encountered in real-world situations. In this context, there is an interest in the development of reliable predictive models of flammability to guide research and regulatory needs. The present work considering CH_2F_2 (R-32) represents part of a larger effort at NIST to characterize and predict the flammability of a range of refrigerant working fluids and their blends[6]: several fluoromethanes: CH_3F, CH_2F_2, CHF_3 (R-41, R-32, R-23) several fluoroethanes: fluoroethane, 1,1-difluoroethane, 1,1,2-trifluoroethane, 1,1,1-trifluoroethane, 1,1,1,2-tetrafluoroethane, pentafluoroethane (R-161, R-152a, R-143, R-143a, R-134a, R-125), several fluoropropenes: 2,3,3,3-tetrafluoropropene, 1,3,3,3-tetrafluoropropene, 2,3,3,3-tetrafluoropropene: (R-1234yf, R-1234ze, R-1243zf), and their mixtures.

In the present paper, we focus on the development of a reliable and fundamentally sound detailed description of the reaction pathways for the decomposition and combustion of CH_2F_2 (difluoromethane, refrigerant R-32) in $CH_2F_2/O_2/N_2$ flames. The required mechanism was assembled

on the basis of the available literature, and rate expressions have been compiled from the literature, estimated, and/or computed with quantum chemical methods/transition state theory. Available rate constant data have then been critically evaluated. The present work presents a broad overview and discussion of many reaction pathways that occur as CH_2F_2 is burned in flames yielding CO_2, HF, and other products. In a recent companion work,[7] two of the present authors have considered in detail an important subset of reactions, H abstractions from the fluoromethanes by the flame radicals H, O, OH, and F, and have evaluated rate constants for the complete homologous series of (fluoro)methanes: CH_4, CH_3F, CH_2F_2, CHF_3, CF_4. We will later summarize some findings from that work, but the reader is referred to the published review for more details of those reactions. We also have a companion paper that validates this model against experimental burning velocities.[8]

The mechanism and recommended rate expressions developed in the present work were used in calculations of freely-propagating premixed flames to model experimental burning velocities derived using a constant volume spherical flame method. The burning velocity experiments and the protocols for their modeling are described elsewhere,[8] but that work does not provide a detailed discussion of the chemistry and kinetics – that is done here. Our modeling accurately predicted (within 3 % to 6 %) the burning velocities for R-32/O_2/N_2 mixtures over a wide range of conditions: oxygen loadings of (21 to 40) %, pressures of P=(1 to 3) bar, initial unburned gas temperatures of T_u=(298 to 400) K, and equivalence ratios of ϕ=(0.8 to 1.3).[8-11] The good agreement of predictions from the model with experimental burning velocities provides strong validation of the kinetics model.

This paper is divided into 4 main sections. The first section provides a general overview of the mechanism and pathways for the destruction and combustion of CH_2F_2 in CH_2F_2/O_2/N_2 flames. The second section provides a more detailed description of the reaction pathways. We would like to emphasize that this present work focuses on the evaluation of rate constants used in the mechanism. A complete description of the mechanism based on experimental determinations and modeling of burning velocities along with a detailed reaction pathway analysis can be found in our experimental validation work.[8] The third section then provides an evaluation and selection of

preferred values for rate constants for the reactions in the mechanism. The final section presents a table with the reactions and rate expressions used in the mechanism. Although the full mechanism is given in the supporting information in Chemkin format,[12] the present work is focused on and discusses only the sub-mechanism and rate expressions for the fluorinated species specific to CH_2F_2. Details of the sub-mechanisms involving hydrogen/oxygen and carbon/hydrogen/oxygen species and reactions can be found elsewhere. [13-15]

Overview of Chemical Kinetic Mechanism

Our present goal was the development of a physically reasonable and quantitatively predictive detailed kinetic model of the chemistry that leads to the destruction and combustion of difluoromethane in $CH_2F_2/O_2/N_2$ flames. As noted earlier, the kinetic mechanism has been tested in a flame model[8] that describes propagation (i.e. burning velocity) of an existing flame through a quiescent homogenous fuel mixture having a defined composition (equivalence ratio) and particular initial pressure and temperature conditions. The flame kinetics model necessarily includes species transport properties, thus allowing radicals in the existing flame to diffuse into the adjacent unburned gas region and initiate the chemistry that ignites that region. The transport properties (see supplementary material) were taken from a number of sources, augmented with our estimations by analogy. [16-20] In our spherically expanding flame experiments that were used to validate the kinetics model, the gas is ignited with a spark in the center of the vessel. The kinetic model here should work adequately for all cases for burning R-32. It is a limited model, however, that will not be sufficient for cases where R-32 is doped into hydrocarbon flames – many additional reactions would then be needed.

The present mechanism is developed for the case where CH_2F_2 is the fuel. We are developing a larger kinetics model with additional reactions that are needed to describe the combustion of other hydrofluorocarbon (HFC) fuels and HFC-doped hydrocarbon flames.[21] The chemistry involves

reactions of species containing carbon, hydrogen, oxygen, and fluorine. By analogy to methane combustion, one expects little formation of species larger than C_2 under conditions of current interest, thus limiting the necessary reactions. For the non-fluorinated species, the base mechanism is simply that of methane combustion, which is well-studied. In developing our model, we therefore held fixed the reactions and rate constants for hydrogen/oxygen and carbon/hydrogen/oxygen species and these were taken from the established literature.[13-15]. This H/O and C/H/O chemistry is not discussed in the present article.

To this relatively well-known C/H/O chemistry, it is necessary to add a fluorocarbon sub-mechanism that describes the breakdown of the fluorinated components. Fortunately, considerable previous work [16, 22-44] on the combustion of fluorinated hydrocarbon systems has established most relevant chemistry at the qualitative level. For instance, one expects unimolecular decomposition of the fuel to be important, as well as radical reactions involving the fuel and major active flame radicals such as H, OH, O, and F.[7] The intermediate fluorocarbon species created by the initial reactions will undergo processes analogous to those of the starting fuel, as well as recombination, disproportionation, and reaction with O_2. On this basis, and following the previous literature, the fluorocarbon sub-mechanism was constructed, and initial rate constants assigned. The kinetics model was developed and validated in an iterative process that is described in detail in our validation paper.[8] In short, premixed flame calculations were carried out with the Cantera software.[45] The most important reactions were determined by calculating the dependence of the computed burning velocities on the rate constants and by carrying out a reaction path analysis using the NIST XSenkplot graphics post-processor.[46] Rate constants for the key reactions so-determined were then critically evaluated as described subsequently and adjusted within their assigned uncertainties to optimize the kinetics model to experimental burning velocity data. As part of this research effort, as mentioned previously, we have published another evaluation paper for H atom abstractions from the fluoromethanes[7] and a validation paper for the kinetics model.[8] Most of the evaluated rate constants presented herein have been derived on the basis of literature data independent of the model validation work. Any adjustments subsequently made during our validation study[8] are noted in the discussions of the individual reactions and in the table of

recommended values provided near the end of the paper. The final kinetics model in Chemkin format is available in the supporting information.

Concurrent with this process, we compiled and updated thermodynamic properties for the fluorinated species. A summary of this information is provided in Table 1, which shows enthalpies of formation, entropies, and heat capacities at standard state. Expanded standard uncertainties U for enthalpies of formation are also provided at the 95 % confidence level (2σ). The expanded standard uncertainties either came from the source cited, or in some cases were assigned by us (Type B uncertainties[47]). Most of the enthalpies of formation were derived from *ab initio* calculations by Ganyecz et al. [48] or from the Active Thermochemical Tables approach by Ruscic and coworkers.[49] For a discussion of systematic uncertainties in the enthalpies of formation for the fluorinated hydrocarbons, see the work at NIST by Paulechka and Kazakov.[50, 51] Thermodynamic polynomials are provided in Supplementary Information (which includes references for the entropies and heat capacities).

In addition, identifiers for species and reaction in this model are provided in the Appendix.

The organization of the rest of the paper is as follows. First, in Section 2, we present in Figures 1, 2, and 3 only the major reactions and characteristic species in the mechanism that control burning velocities and/or combustion pathways. Next, in Section 3, we identify all of the reactions that form and destroy all of the species in the mechanism (whether or not the species and reactions control burning velocities and whether or not the species and reactions are important, secondary, minor, or negligible). Following that, in Section 4, we evaluate the rate constants for all of these reactions (again, whether or not they control burning velocities or are important, secondary, minor, or negligible). Finally, in Section 5, we present rate expressions for all of these reactions. We emphasize that the present work describes reaction pathways in CH_2F_2 combustion and the derivation and evaluation of physically-reasonable rate constants for the considered reactions on the basis of experimental and theoretical data from the literature, sometimes as augmented by our

own computations and optimization work. Uncertainties ranges are given in all cases. For more details regarding the development, validation, and optimization of this kinetics model, including a more detailed reaction pathway analysis, see our companion paper.[8]

As summarized in Figure 1 and Figure 2, our reaction path analysis shows that the decomposition and combustion of CH_2F_2 in a propagating flame proceeds through two primary pathways whose relative importance is different in the pre-flame initiation and flame combustion zones. Other fluorinated hydrocarbon reactions play minor roles but contribute less than 5 % to the computed burning velocities over the conditions studied. Per previous discussion, note that this analysis does not include reactions of pure hydrocarbons (C/H), oxidized hydrocarbons (C/H/O), or species that contain only hydrogen-oxygen (H/O) or hydrogen-oxygen-fluorine (H/O/F).

In Figure 1 (low temperature), the very important CHF species is created by $CH_2F_2 + OH \rightarrow CHF_2 + H_2O$ followed by the product CHF_2 destruction via $CHF_2 + H \rightarrow CHF + CHF$. Then, CHFO is created through the important reaction $CHF + O_2 \rightarrow CHFO + O$ producing the "initial" radical O atom that starts the chemistry with the CHF_2 created through H atom abstraction from CH_2F_2 by recycled OH radicals. OH is important because it is recycled through a two-step reaction, and contributes significantly to radical chain propagation: $CH_2F_2 + OH \rightarrow CHF_2 + H_2O$ followed by $CHF_2 + O_2 \rightarrow CF_2O + OH$. Overall, this relatively quick two-step reaction can be written as $CH_2F_2 + O_2 \rightarrow CF_2O + H_2O$, thus converting the starting fuel to a fluorinated oxidized closed-shell intermediate and forming water, which is a final thermodynamically favorable end-product. The OH radicals driving this chemistry come from the radical initiation and chain branching steps $CHF + O_2 \rightarrow CHFO + O$ followed by $HO_2 + H \rightarrow 2\ OH$. The reaction $HO_2 + O \rightarrow OH + O_2$ is also important. The creation and destruction of both CHFO and HO_2 (both species have a maximum here) are indicators of this low temperature initiation zone where O atoms are produced (see Figure 3). We note that radicals in the initiation chemistry are also produced as a consequence of diffusion of H atoms from the flame zone.

In Figure 2, the CHF_2 at high temperatures in the combustion zone is created through H atom abstraction from CH_2F_2 by flame radicals, $CH_2F_2 + X \rightarrow CHF_2 + HX$ (X = H, O, OH, F). There are two sub-zones here: a region where there is exponential radical growth at about 1400 to 1700 K and a flame zone at about 1700 K to 1900 K at initial conditions: air (21 % O_2), P = 1 bar, and T_u = 298 K. The temperature ranges vary somewhat with conditions, because temperatures in the flame zone are higher for higher O_2 loadings, pressures, and initial temperatures.

The two sub-zones are clearly evident in Figure 3 where we present concentration profiles for the reactant CH_2F_2 and the important HFC intermediates CHFO and CHF_2 along with the H/O flame radicals HO_2 and OH. The concentration profile of HO_2 is bimodal with the first maximum an indicator of the initiation zone and the second maximum an indicator of the flame zone. Concurrent with the bimodal HO_2 profile is CHFO, an indicator of the initiation zone, and CHF_2, an indicator of the exponential radical growth and flame zones. We note that the concentration profile for CHF is not illustrated in this figure, but CHF is an important intermediate between CH_2F_2 and CHFO in the initiation zone being formed slowly from CH_2F_2 and then destroyed quickly to form CHFO. The reaction sequence here is: $CH_2F_2 + OH \rightarrow CHF_2 + H_2O$ plus $CHF_2 + H \rightarrow CHF + HF$ (two slow rate determining steps) followed by $CHF + O_2 = CHFO + O$ (relatively fast). Concurrent with the second HO_2 phase is formation of CHF_2, which is produced during the exponential radical growth phase – this phase is indicated in Figure 3 by the exponential growth of the flame radical OH.

The chemistry in the high temperature combustion pathway is much different than the low temperature zone consisting of irreversible reactions with no recycling of hydrogen/oxygen species – it is all "downhill" to CO_2. As discussed above, the creation and destruction of CHF_2 along with the second HO_2 profile are indicators of this pathway. In addition, CH_2F_2 also begins to decompose via unimolecular decomposition: $CH_2F_2 + M \rightarrow CHF + HF + M$. The destruction of CH_2F_2 via abstraction reactions by flame radicals ($CH_2F_2 + X \rightarrow CHF_2 + HX$) leads to the formation of CF_2O, while the destruction via unimolecular decomposition leads to the formation of CHFO; both leading to the products CO and then CO_2.

The relative importance of each abstraction channel (X = H, O, OH, F) varies with conditions (O_2 concentration, pressure, temperature, and equivalence ratio). Because flames of fluorinated fuels are hydrogen-poor relative to hydrocarbon flames, F atoms are prevalent in the combustion zone (comparable in concentration to H atoms). These F atoms are produced by the reactions CFO + M → CO + F + M and HF + OH ↔ H_2O + F. The former channel is the largest source of F and is irreversible because of the thermodynamics. In contrast, the latter channel is highly reversible and nearly equilibrated; it is the primary reaction controlling F atom concentrations.

As discussed above, the kinetics model was developed and validated in an iterative process that is described in detail in our validation paper.[8] The most important reactions were determined by determining the dependence of the computed burning velocities on the rate constants. A number of the rate constants were adjusted within their assigned uncertainties to optimize the kinetics model to experimental burning velocity data. Our reaction path analysis (see Figure 4) indicates that the two most important HFC reactions controlling burning velocities are the unimolecular decomposition CH_2F_2 + M → CHF + HF + M and the subsequent radical initiation step CHF + O_2 → CHFO + O. For the first reaction CH_2F_2 + M → CHF + HF + M, the change in the computed burning velocity S_u with rate constant k, i.e. in $\Delta S_u'/\Delta k'$, where $\Delta S_u' = \Delta S_u/S_u$ and $\Delta k' = \Delta k/k$, is relatively insensitive to equivalence ratio: increases are on the order of +20 % to +25 % at low (0.8) to high (1.3) equivalence ratios, respectively. For the second reaction CHF + O_2 → CHFO + O, $\Delta S_u'/\Delta k'$ changes significantly increasing on the order of about +5 % to about +15 % at low and high equivalence ratios, respectively. These magnitudes are illustrated in Figure 4. There are three other HFC reactions that contribute to changes to burning velocities. CHF_2 + O_2 → CF_2O + OH is largely insensitive to equivalence ratio with $\Delta S_u'/\Delta k'$ increasing about +5%. The other two of these reactions actually inhibit flame propagation. For CH_2F_2 + H → CHF_2 + H_2, flame speeds decrease with $\Delta S_u'/\Delta k'$ about -5 % and also for CHF + CHF → C_2HF + HF flame speeds decrease with $\Delta S_u'/\Delta k'$ changing from about 0 % to about -5 % at low to high equivalence ratios, respectively. The first reaction CH_2F_2 + H → CHF_2 + H_2 inhibits flame propagation, because it reduces H atom (and OH and HO_2 radical) concentrations which are important for flame propagation. The latter reaction CHF + CHF → C_2HF + HF (where we assigned an upper limit estimated rate constant) is a termination step. All of these changes in flame

speed quoted here are rough values and do change somewhat with conditions (O_2 loadings, pressures, and initial temperatures).

Overall, the chemistry of reaction consumes CH_2F_2 and O_2 leading to the generation and recycling of O atoms and OH radicals and flame propagation through the key hydrofluorocarbon intermediates CHF and CHF_2. This chemistry is discussed in more detail now.

The two primary destruction pathways for CH_2F_2 are 1) the unimolecular elimination of HF to form CHF and 2) H abstraction from difluoromethane by flame radicals to form CHF_2

1) $CH_2F_2 + M \rightarrow CHF + HF + M$

2) $CH_2F_2 + X \rightarrow CHF_2 + HX$ (X=H, O, OH, F)

The relative importance of the two paths varies significantly with conditions: the rate of unimolecular HF elimination is close to the high-pressure limit at the lower temperatures of the pre-flame zone, but is in the fall-off regime in the combustion zone, making this pathway somewhat dependent on the system pressure and temperature. Complicated behavior is similarly found for the bimolecular abstraction pathways, for which rates strongly depend on radical concentrations, and therefore vary substantially with temperature and the stage of combustion. The first pathway, unimolecular decomposition (and subsequent reactions), largely drives the chemistry in the lower temperature pre-flame zone where radical concentrations are relatively low. This chemistry drives ignition and controls burning velocities, while the abstraction pathways (and subsequent reactions) complete the combustion once the flame is established and have little direct impact on burning velocities. Radical concentrations progressively build throughout the lower temperature pre-flame zone due to radical propagation and branching. Eventually, radical-based decomposition of CH_2F_2 becomes competitive with unimolecular decomposition at a point that varies with the temperature,

pressure, and mixture composition. Note that unimolecular decomposition of CH_2F_2 is important in both the pre-flame and flame zones.

Our simulations show that there are two reaction pathways in the pre-flame zone that significantly impact burning velocity. The first, and most important, is initiated by the unimolecular decomposition of CH_2F_2 and the second involves H abstraction from CH_2F_2 by OH radicals. These initial steps are followed by the reaction of the intermediate decomposition products CHF and CHF_2, respectively, with the reactant O_2, producing the important flame radicals O and OH, respectively (which contribute to radical chain branching and flame initiation).

$$CH_2F_2 + M \rightarrow CHF + HF + M$$

$$CHF + O_2 \rightarrow CHFO + O$$

and

$$CH_2F_2 + OH \rightarrow CHF_2 + H_2O$$

$$CHF_2 + O_2 \rightarrow CF_2O + OH$$

Note that H abstraction from CH_2F_2 by H atoms is important in the pre-flame zone. As noted above, it actually inhibits burning velocities due to consumption of H atoms, which otherwise would contribute to chain branching. The latter reaction between CHF_2 and O_2 is a radical combination followed by an isomerization (termed QOOH chemistry: $R^* + O_2 \rightarrow ROO^* \rightarrow {}^*QOOH$) followed by beta scission of OH. It is highly exothermic, essentially proceeding with no barrier.

The reactions above are the most sensitive reactions controlling burning velocity in this system. The set of reaction pathways involving fluorinated hydrocarbons responsible for radical initiation and propagation can be described as:

$CH_2F_2 + M \rightarrow CHF + HF + M$ (initiation of chemistry)

$CHF + O_2 \rightarrow CHFO + O$ (first radical)

$CH_2F_2 + O \rightarrow CHF_2 + OH$ (initiation of OH)

$CHF_2 + O_2 \rightarrow CF_2O + OH$ (production of OH, first step in chain cycle)

$CH_2F_2 + OH \rightarrow CHF_2 + H_2O$ (destruction of OH, second step in chain cycle)

As previously noted, the flame model includes species transport properties, thus allowing radicals in the existing flame to diffuse into the adjacent unburned gas region and initiate the flame chemistry. Burning velocities in this flame are most sensitive to the first two fluorinated hydrocarbon reactions shown above. The last three reactions have much lower sensitivities because their rates are sufficiently high that they are not rate determining. Nonetheless, they are important to complete the chemistry to products. The last two steps are involved in recycling the radical OH and are responsible for initiating the build-up of radicals in the pre-flame zone along with the H/O chemistry. Overall, the two steps add up to

$CH_2F_2 + O_2 \rightarrow CF_2O + H_2O$

while recycling OH radicals (through H/O chemistry involving H, O, OH, HO_2) and contributing to H, O, and OH radical propagation.

Although the unimolecular decomposition step has a larger impact on flame speeds compared to other reactions (by a factor of two or more), the subsequent reaction $CHF + O_2 \rightarrow CHFO + O$ is a necessary component of the process in that it is the primary radical initiation step in this system (forming O atoms) and is the primary pathway for the destruction of O_2.

The unimolecular decomposition pathway remains important in the combustion zone, but the abstraction pathways, of limited importance in the pre-flame zone, play an increasingly larger role.

$CH_2F_2 + X \rightarrow CHF_2 + HX$ (X=H, O, OH, F)

followed by

$CHF_2 + O_2 \rightarrow CF_2O + OH$

As previously noted, the importance of each abstraction channel varies with conditions.

The initial decomposition of CH_2F_2 produces the important intermediates CHF and CHF_2 which react with O_2 resulting in CHFO and CF_2O, respectively. These short-lived species are converted to final combustion products CO and CO_2 and to HF via:

$$CHFO + M \rightarrow CO + HF + M$$

$$CF_2O + H \rightarrow CFO + HF$$

$$CFO + M \rightarrow CO + F + M$$

$$CO + OH \rightarrow CO_2 + H$$

All other chemistry (involving fluorinated species) is secondary to controlling flame velocities. We note that there are other reactions of secondary importance, but necessary, because they provide paths to complete combustion. All of the reactions included in the kinetics mechanism are described below in Section 3 Reaction Pathways Description.

In summary, based on our reaction path analysis, we find there are two (quasi-sequential) regions for the destruction and combustion of CH_2F_2 in $CH_2F_2/O_2/N_2$ flames: a pre-flame initiation zone and a flame combustion zone. These are illustrated in Figures 1, 2, and 3, and described in detail above.

Reaction Pathways Description

In the previous section, we provided an overview of the mechanism. This present section provides a more detailed look at the formation and destruction pathways of specific intermediates in the conversion of reactants (CH_2F_2, O_2) to products (CO_2, CO, H_2O, HF). The overall reaction pathways

are shown in Figure 1 and Figure 2 and are discussed above for low temperature initiation chemistry and high temperature flame chemistry, respectively.

CH_2F_2

In the combustion zone, the most important destruction pathway of CH_2F_2 is unimolecular decomposition. Under stoichiometric and rich conditions, this pathway contributes about 40 % to destruction of CH_2F_2, while under lean conditions this is reduced to about 25 %. (Note these values are integrated total destruction, not changes in flame speeds with changes in rate constants, $\Delta S_u'/\Delta k'$ a quantity discussed above). These values vary with oxygen loadings, pressures, and T_u. The balance of the destruction occurs via H abstractions by H, O, OH, and F. Under lean conditions (high relative oxygen), the abstraction reactions by OH and O each contribute about (20 to 40) % more to decomposition than does the unimolecular decomposition pathway. Note that these percentages are rough values that change with conditions. Also note that although these reactions lead to complete combustion, they do not control the burning velocities (i.e., $\Delta S_u'/\Delta k'$). The burning velocities are primarily determined by reactions in the pre-flame zone, where the unimolecular decomposition of CH_2F_2, the reaction of CHF with O_2, and H abstraction by H atom are most important.

Destroyed: $CH_2F_2 + M \rightarrow CHF + HF + M$

$CH_2F_2 + X \rightarrow CHF_2 + HX$ (X = H, O, OH, F)

CHF

Unimolecular decomposition of CH_2F_2 creates about 70 % of CHF in the flame, largely independent of the equivalence ratio. The major secondary source is reaction of CHF_2 with H atoms. Destruction of CHF via reaction with O_2 accounts for about (55 to 70) % of the respective total loss under rich to lean conditions, respectively. Again, note that these percentages are rough values that change with conditions (as will all others quoted subsequently). Secondary loss is mainly through reactions with

O and H atoms. Note that the reaction with O_2 dominates destruction of CHF in the pre-flame zone where burning velocities are controlled.

Formed: $CH_2F_2 + M \rightarrow CHF + HF + M$

$CHF_2 + H \rightarrow CHF + HF$

Destroyed: $CHF + O_2 \rightarrow CHFO + O$

$CHF + O \rightarrow CO + HF$

$CHF + H \rightarrow CH + HF$

$CHF + H \rightarrow CF + H_2$

O_2

The primary pathway for the destruction of O_2 is reaction with CHF and with H. In rich flames, these two channels are roughly equal (35 to 40) %, while in lean flames the $O_2 + H \rightarrow OH + O$ channel is about twice that of the $CHF + O_2 \rightarrow CHFO + O$ channel – about 45 % compared to 20 %, respectively. Note that the $CHF + O_2$ pathway is very important, not only for overall combustion, but especially in the pre-flame stage that controls burning velocities. Secondary channels for destruction of O_2 are its reaction with CHF_2 and its reaction with H to form HO_2.

Destroyed: $CHF + O_2 \rightarrow CHFO + O$

$O_2 + H \rightarrow OH + O$

$CHF_2 + O_2 \rightarrow CF_2O + OH$

$O_2 + H \rightarrow HO_2$

CHF_2

CHF_2 is formed primarily via abstraction of H from CH_2F_2 by active radicals in the system, a mix of H, O, OH, and F. Abstractions by O and OH dominate under lean conditions (~70 %), while the reactions with H and F become increasingly important under stoichiometric and rich conditions. Destruction

of CHF_2 is primarily via the quick reactions with H, O, and OH radicals at high temperatures. Although reaction of CHF_2 with O_2 makes only a small contribution to the flux of CH_2F_2, this is an important reaction at low temperatures that impacts burning velocities because of its role in the pre-flame region (see Figures 1 and 3 which illustrate this). The combination of CHF_2 radicals is of minor importance.

Formed: $CH_2F_2 + X \rightarrow CHF_2 + HX$ (X = H, O, OH, F)

Destroyed: $CHF_2 + O_2 \rightarrow CF_2O + OH$ (pre-flame)

$CHF_2 + H \rightarrow CHF + HF$ (flame)

$CHF_2 + O \rightarrow CF_2O + H$ (flame)

$CHF_2 + OH \rightarrow CHFO + HF$ (flame)

$CHF_2 + CHF_2 \rightarrow CHFCF_2 + HF$ (flame)

CHFO

CHFO is formed from the initial CH_2F_2 decomposition intermediates CHF and CHF_2 and then destroyed quickly via unimolecular decomposition – leading to CHFO being present in near steady state concentrations (destroyed as fast as it is formed).

Formed: $CHF + O_2 \rightarrow CHFO + O$

$CHF_2 + OH \rightarrow CHFO + HF$

Destroyed: $CHFO + M \rightarrow CO + HF + M$

CF_2O

CF_2O is formed from CHF_2 via reaction with O and O_2 (about 75 % and 25 %, respectively). It is destroyed primarily (85 to 90) % via reaction with H atoms and secondarily through unimolecular

decomposition. Its reaction with H_2O was found to be negligible using the rate expression of Zachariah et al. [53, 54]

Formed: $CHF_2 + O \rightarrow CF_2O + H$

$CHF_2 + O_2 \rightarrow CF_2O + OH$

Destroyed: $CF_2O + H \rightarrow CFO + HF$

$CF_2O \rightarrow CFO + F$

CFO

CFO is primarily formed (70 to 75) % through decomposition of CF_2O by F abstraction by H atoms, and secondarily via unimolecular decomposition of CF_2O as well as the reaction of the CF radical with the reactant O_2. It is primarily destroyed quickly via unimolecular decomposition (85 to 90) % and secondarily via reaction with O and OH radicals.

Formed: $CF_2O + H \rightarrow CFO + HF$

$CF + O_2 \rightarrow CFO + O$

Destroyed: $CFO + M \rightarrow CO + F + M$

$CFO + O \rightarrow CO_2 + F$

$CFO + OH \rightarrow CO_2 + HF$

CO

CO and CO_2 are final products in combustion with CO being a product under incomplete combustion (not fully converted to CO_2 due to insufficient oxygen). The primary pathway for formation of CO is from the unimolecular decomposition of CFO; the contribution of this pathway varies from about 75 % (lean) to 50 % (rich). Secondary reactions producing CO are the unimolecular decomposition of HCO and reaction between CHF and O atoms. The primary destruction pathway for CO is, of course, its reaction with OH to form CO_2.

Formed: $CFO + M \rightarrow CO + F + M$

$HCO + M \rightarrow CO + H + M$

$CHF + O \rightarrow CO + HF$

Destroyed: $CO + OH \rightarrow CO_2 + H$

There are a few other species of secondary importance that have little-to-no impact on burning velocities, but

are necessary to provide a complete path for combustion.

CF_2

The two primary reactions contributing to the formation of CF_2 are $CHF_2 + F$ and $CF_2O + H$. A secondary source is $CF + HF$. The $CF_2O + H$ channel becomes more important under rich conditions. CF_2 is the quickly destroyed via reaction with both O and OH radicals.

Formed: $CHF_2 + F \rightarrow CF_2 + HF$

$CF_2O + H \rightarrow CF_2 + OH$

$CF + HF \rightarrow CF_2 + H$

Destroyed: $CF_2 + O \rightarrow CFO + F$

$CF_2 + OH \rightarrow CF_2O + H$

CF

CF is primarily formed from CHF + H, this reaction being near equilibrium. It is destroyed quickly mainly via reaction with O_2, which contributes between 50 % and 70% under rich and lean conditions, respectively. Secondary reactions destroying CF are its reactions with O and OH radicals.

Formed: $CHF + H \rightarrow CF + H_2$

Destroyed: $CF + O_2 \rightarrow CFO + O$

$CF + O \rightarrow CO + F$

$CF + OH \rightarrow CO + HF$

CH_2O

Interestingly, CH_2O in this CH_2F_2/O_2 flame is primarily formed (85 %) from the reaction of CHF with H_2O and is destroyed via H abstractions by the radicals H, O, and OH. Although CH_2O is an important species during combustion (leads quickly to HCO, CO, then CO_2) and this reaction is the primary reaction forming CH_2O, this reaction does not contribute at all to changes in burning velocities.

Formed: $CHF + H_2O \rightarrow CH_2O + HF$

Destroyed: $CH_2O + X \rightarrow HCO + HX$ (X = H, O, OH)

C_2HF

C_2HF (fluoroethyne) is formed following the self-recombination of CHF to form a chemically-activated difluoroethene that then decomposes by eliminating HF. It is then quickly destroyed via reaction with H atoms.

Formed: $CHF + CHF \rightarrow C_2HF + HF$

Destroyed: $C_2HF + H \rightarrow C_2H_2 + F$

(*Z*)-CHFCHF

(*Z*)-CHFCHF (1,2-difluoroethene) is formed via insertion of CHF into a C–H bond in the reactant CH_2F_2 forming a chemically-activated fluorinated ethane which then decomposes eliminating HF. **(*Z*)-**CHFCHF is then quickly destroyed through reaction of O atoms.

Formed: $CH_2F_2 + CHF \rightarrow$ **(*Z*)-**CHFCHF + HF

Destroyed: ***(Z)-***$CHFCHF + O \rightarrow CH_2F + CFO$

Reaction Rates Evaluation

In this section we present the reaction rate expressions that we have employed and discuss their sources. Reaction enthalpies quoted in the evaluations refer to standard state values at 298.15 K. In general, rate expressions were chosen through an iterative process that consisted of a compilation and evaluation of experimental and computed rate constants from the literature, with extension via our own quantum chemical calculations (G3B3)[55] of transition state structures and energies. Where necessary, RRKM/Master Equation modeling using the program ChemRate [56] was employed. For discussions of RRKM reaction rate theory see articles by Marcus and others. [57] [58] [59] [60] [61] Rate expressions obtained on this basis were then used in simulations of premixed flames where, through use of reaction path analysis , the kinetics model was refined (reactions added or removed) and a few important rate expressions were adjusted within their uncertainty limits to achieve best agreement between the experimentally-derived and computed burning velocities over a wide range of experimental conditions: oxygen mole fractions of (21 to 40) %, total pressures P = (1 to 3 bar), unburned gas temperatures T_u = (298 to 400) K, and equivalence ratios ϕ = (0.8 to 1.3).

We first discuss the individual rate expressions, followed by table of rate expressions for the reactions. This section is organized as follows. We begin with an overview of the hydrogen/oxygen/carbon chemistry utilized in this work, then describe the hydrogen/oxygen/fluorine chemistry, and finally the fluorinated hydrocarbon chemistry in the order CH_2F_2, CHF_2, CHF, CF_2, CF, CF_2O, CHFO and CFO. Unless otherwise noted, reaction energetics pertain to ground state species.

Please note that throughout this paper, we refer to uncertainty factors (*f*) for rate constants, a standard parameter in chemical kinetics. For example, *f* = 2 is an uncertainty of a factor two (i.e. *k* is between *k*/2 and 2**k*). Generally, we consider our assigned uncertainty factors *f* to be at the 95 % confidence level.

Hydrocarbons and Oxidized Hydrocarbons

For the hydrogen-oxygen, hydrocarbon, and oxidized hydrocarbon chemistry, we have largely used the rate expressions from GRI-Mech 3.0 [13], except for the rate expression for $H+O_2(+M) \rightarrow HO_2(+M)$, where the parameters from JetSurf 2.0 [14] were used and judged to provide a better description of the fall-off behavior under lean conditions. Under our conditions, the JetSurf 2.0 formulation provided burning velocities that were nearly identical to those obtained using the various rate expressions recommended by Dryer and coworkers [15], Konnov and coworkers [62], and Frenklach and workers [63].

Hydrogen/Oxygen/Fluorine Species

HF is formed via a half a dozen or so reactions and is then destroyed primarily through its reversible reaction with OH to form water and F atoms. This results in an approach to equilibrium for $HF + OH \leftrightarrow H_2O + F$, particularly at higher temperatures and in the later stages of combustion. In the combustion regime, F atom concentrations typically reach a steady state where production processes balance with the rapid reaction of F with the CH_2F_2 fuel, a reaction that is a major source of HF. In the fuel-depleted post-combustion gases, decomposition of CFO to CO + F is an important direct source of F, whereas the primary sink of F is the reversible reaction with H_2O. The concentration of F scales inversely with the availability of hydrogen under the conditions considered. Key processes governing the kinetics and determining the fluorine reservoir species under specific conditions are the reactions of F and HF with hydrogen-oxygen species. Our rate expressions for reactions involving F and HF with hydrogen-oxygen species are our fits to experimental data from the literature. These often involve extrapolations from results obtained at lower temperatures. All of the reactions below (H_2O, H_2, OH, HO_2) + F contribute to the reaction flux.

$H_2O + F \longrightarrow OH + HF$

This reaction is exothermic by about 73 kJ mol^{-1}. Rate constants have been measured at low temperatures (243 to 369) K by Walther and Wagner in 1983, [64] at (240 to 373) K by Stevens et al. in 1989, [65] at 298 K by Frost et al. in 1986,[66] and at 294 K by Anastasi et al. in 1991.[67] Nguyen et al. later in 2013 computed rate constants using semi-classical transition state theory.[68] In 1985, Leroy at al. reported a rate constant at 1050 K using transition state theory based on an ab initio transition state, but it is about a factor of 20 lower than the recommended value.[69] More recently in 2019, Li computed a potential energy surface for this reaction and provided rate constants at (200 to 400) K.[70] Zhang et al. just recently in 2021 computed a potential energy surface, but provided no rate constants.[71] We employ in our kinetics model a rate expression that is a fit to the rate constants of Nguyen et al. (given in their supplementary material) over the temperature range (500 to 2000) K. Note that there is a negative temperature dependence to the rate constants from the work of Nguyen et al. below about 400 K (our recommended rate expression does not include this range). The rate expression recommended here agrees well (within 20 % to 25%) at (200 to 400) K with the experimental measurements of Frost et al. and by Stevens et al, and with the calculations of Nguyen et al. and Li (see Figure 5). The uncertainty factor in the recommended rate constant for this reaction at flame temperatures is low (f < 1.4), because the rate constant is relatively insensitive to temperature (it has an effective temperature-dependence of only about 15 kJ mol^{-1}, that is, $k \propto \exp(-15 \text{ kJ mol}^{-1}/RT)$.

$H_2 + F \longrightarrow HF + H$

This reaction is exothermic by about 134 kJ mol^{-1}. The work of Persky and Kornweitz in 1997[72] provides evaluated rate constants for this reaction at low temperatures (190 to 376) K based on the measurements of Wurzberg and Houston,[73] Clyne and Hodgson,[74] and Stevens et al.[65] (see Figure 6). In other work, the rate constants in similar temperature ranges from the work of Igosin et al.[75] agree well with the recommendation of Persky and Kornweitz. The rate constant at room

temperature reported by Fasano and Nogar[76] agree well with the recommendation of Persky and Kornweitz. The rate constants of Homann et al.[77] show a much stronger temperature dependence and are about a factor of 1.5 low at 298 K, extrapolating to about 20 % higher at higher temperatures. The rate constants in the range 295 K to 765 K from Heidner et al.[78] are about 40% larger than other measurements, as is the rate constant reported by Preses et al.[79] at about 400 K. Kompa and Wanner[80] report a value at room temperature that is about a factor of 2.5 high, the room temperature value of Goldberg and Schneider[81] is about a factor of 1.5 high. The rate constants reported by Ioffe et al.[82] have a much stronger temperature dependence with rate constants lower by factors of 1.5 to 3.0 in the range 293 K to 700 K.

Very recently (2021), Bedjanian [83] measured the rate of this reaction over wide temperature range (220 K to 960 K) and the values agree with the recommendation of Perksy and Kornweitz within about 10 % at low temperatures (200 K to 400 K). The rate constants of Bedjanian show little curvature (non-Arrhenius behavior) at higher temperatures (400 K to 960 K), while one expects some curvature because of changes in heat capacity and entropy. In addition, the entropic contribution should change because of the spin-orbit splitting of F atoms in the ground state (see short discussion below). Sun and Zhang,[84] De Fazio et al. [85], Chen et al. [86], and Moix and Huarte-Larranaga [87] have all performed trajectory calculations on *ab initio* potential energy surfaces, but unfortunately, only predicted rate constants at lower temperatures. Wang et al. have used potential energy surfaces[88] and Steckler and Truhlar[89] have used *ab initio*/transition state theory to predict rate expressions at slightly higher temperatures (300 K to 600 K and 159 K to 765 K, respectively). The rate constants predicted by Wang et al. are only about 5% lower than the recommended values of Persky and Kornweitz. Steckler and Truhlar's calculations are the only ones that predict rate constants at higher temperatures (765 K) – from their data we compute a temperature exponent of about n=1.0 – corresponding to a rate constant that is about 2 times larger near 765 K than if extrapolated using a simple Arrhenius fit to the lower temperature data. In other work, Aquilanti et al. have computed a potential energy surface and predicted rate constants at (200 to 335) K, which are in good agreement with the experimental values.[90] In short, the rate constants measured at low temperatures need to be extended to higher temperatures relevant to combustion.

This is a complicated reaction because tunneling, resonance phenomenon, electronic non-adiabatic transitions, multiple potential energy surfaces, changes in barrier height due to linear vs. bent transition states, contribution from the rate constant in ν=1 ($\Delta\nu$ =3800 cm^{-1}), quantum dynamical effects, movement of the turning point along the reaction coordinate, and the spin-orbit splitting (400 cm^{-1}) of F atoms in the ground state ($^2P_{3/2}$ and $^2P_{1/2}$) will contribute to curvature in the temperature-dependence of the Arrhenius rate expression. These complications are discussed in more detail in the theoretical references provided above (there are many other theoretical references for this reaction that are not cited here). In fact most of the theoretical works cited here point out that future work should address the rate constants at higher temperature.

Giving the lack of detailed measurements or *ab initio* and trajectory calculations at combustion temperatures, we adopted a temperature exponent (T^n) of n = 0.7 and used this in a modified-Arrhenius fit to the data recommended by Persky and Kornweitz. [72] The uncertainty factor for this reaction at flame temperatures is low (f = 1.4) and was assigned based on a range of estimated temperature exponents n = (0.4 to 1.0).

$OH + F \rightarrow O + HF$

This process is highly exothermic (about 140 kJ mol^{-1}) and is a radical disproportionation involving the very reactive F atom, and thus should be essentially a barrierless reaction. [91] Rate constants were been determined by Walther and Wagner in 1983 [64] at low temperatures (240 to 370) K. Although the rate constants are relatively large, they still need to be extended to combustion temperatures. Gomez-Carrasco et al. in 2004 [91] reported a computed *ab initio* potential energy surface and simulated the reaction using quasi-classical trajectory calculations. Their calculations generally agree with the experimental data. Unfortunately, they did not compute rate constants at the higher temperatures relevant to combustion. We used a temperature exponent of (n=0.5) to derive a rate expression that fits the low temperature experimental data of Walther and Wagner and

extends the rate expression to combustion temperatures. Based on a range of assumed temperature exponents (0.3 to 1.0), we estimated an uncertainty factor of about f = 1.3. We note that the rate constants recommended here are about a factor of (2.5 to 3.0) smaller than our previous recommendation in 1995, which was an upper limit estimate.[44]

$HO_2 + F \rightarrow O_2 + HF$

This is a very fast reaction. We fit the rate constant of $5x10^{13}$ cm^3 mol^{-1} s^{-1} at room temperature suggested by Walther and Wagner [64] to a rate expression with temperature factor of n=0.5 and E=0; this increases the rate constant to about $1x10^{14}$ cm^3 mol^{-1} s^{-1} at flame temperatures and we estimate an uncertainty factor of about f = 1.4. This is a radical-radical reaction with F atoms (extremely reactive), and there should be no barrier to reaction – indeed, at room temperature the rate constant is already large.

Fluorinated Hydrocarbons: CH_2F_2

$CH_2F_2 + M \rightarrow CHF + HF + M$

Unimolecular decomposition of CH_2F_2 is the most important reaction controlling burning velocities in R-32 mixtures. It is (1.5 to 2.0) times as important as the subsequent reaction between the intermediate CHF and O_2 in the reactant gas, and at least (4 to 5) times as important as other reactions (see for example, Figure 4 above). Rate constants for the decomposition of CH_2F_2 have been reported by three groups: Politanskii and Shevchuk[92], Cobos et al.[93], and Matsugi and Shiina[94] (see Figure 7).

In flow reactor studies at atmospheric pressure, Politanskii and Shevchuk in 1968 measured rates of decomposition of both CH_2F_2 and CHF_3 by using gas chromatography to follow loss of starting

compound. Although their relative rates are reasonable based on computed barriers from our *ab initio* calculations, we did not directly employ their rate constants for CH_2F_2 for two reasons. First, their measurements are at relatively low temperatures and a direct extrapolation would not account for the substantial pressure falloff that is expected under our conditions. Second, their use of a flow reactor and high concentrations of CH_2F_2 (about 10 %) are likely to create conditions where secondary reactions and radical chains are important, thus potentially leading to apparent unimolecular rate constants that are too large.

More recently, Cobos et al. in 2017 [93] reported an indirect determination of the rate of $CH_2F_2 + M \rightarrow CHF + HF + M$ from shock tube studies at (1400 to 1800) K. They monitored production of CF_2, a secondary product, and then used a quantum chemical model and various mechanistic assumptions to derive rate constants that fit these data. Pressure falloff of the rate constants were described with Troe parameters [95] and they provided limiting high- and low-pressure rate expressions based on their calculations. We did not use their expressions because of the indirect nature of their measurements. A better set of data to utilize are the measurements by Matsugi and Shiina [94] (see discussion below), which are more direct and were made at conditions more relevant to our experimental conditions.

Matsugi and Shiina reported CH_2F_2 decomposition rate constants determined using real-time laser absorption measurements to follow HF production in shock tube pyrolysis experiments. Their measurements were made in argon at total pressures of about 1 bar at temperatures of (1577 to 2214) K, conditions where the reaction is well into the pressure falloff-regime. They calculated the pressure and temperature dependence of the rate constant using RRKM/Master Equation modeling using an *ab initio* transition state and found good agreement with their experiments, with measured rate constants being about 10 % and 40 % lower than their modeled values at the lower and upper ends of their temperature range, respectively. For comparison, our suggested rate constants, derived independently as discussed below from "best fits" to reproduce the measured burning velocities, have a similar quality match to the experimental data: after changing the bath gas in our RRKM model from N_2 to argon, our results are about 25 % lower and 10 % higher at 1800 K and 2200

K, respectively, than the measured values. Overall, our RRKM/Master Equation model produces rate constants lower than those of the Matsugi and Shiina model by (10 to 15) % near 1800 K and (30 to 35) % near 2200 K. This is good agreement, considering the various experimental and modeling uncertainties.

We used an iterative process to develop a parameterized Troe-format pressure-dependent rate expression that fits our burning velocity data and is consistent with our RRKM/Master Equation model implemented in ChemRate [56] and utilizing an *ab initio* (G3B3)[55] transition state. We began by estimating CH_2F_2 decomposition rates by combining measured decomposition rates for the analogous reaction $CHF_3 + M \rightarrow CF_2 + HF + M$ from the shock tube work of Schug et al. [96] with the relative rate expressions for the decompositions of CHF_3 and CH_2F_2 as determined by Politanskii and Shevchuk.[92] From figures in the work of Schug et al. , we extracted rate parameters ($A = 4.9 \times 10^{10}$ s^{-1}, $E_a = 230.8$ kJ mol^{-1}) and ($A = 5.6 \times 10^{11}$ s^{-1}, $E_a = 267.2$ kJ mol^{-1}) at 1 bar and 10 bar, respectively, where the rate constant is given by $k = A \exp(-E_a/RT)$. From the work of Politanskii and Shevchuk, we estimated relative rate parameters of $A_{CH2F2}/A_{CHF3} = 1.33$ and $\Delta E_a = +11.8$ kJ mol^{-1}. This initial estimate gave generally satisfactory agreement (within 20 %) between measured and computed burning velocities under the conditions: P=1 bar, initial temperature T_u=298 K, equivalence ratio ϕ=(0.8 to 1.3). However, there are significant uncertainties in this comparison. First, although radiation (heat) loss in the flame can change the burning velocity by up to (10 to 15) %, the exact heat loss in the experiments cannot be readily determined. Second, from the work of Schug et al., we know that CH_2F_2 decomposition is in the pressure falloff-regime. Third, the collision efficiency of CH_2F_2 is unknown, but its value impacts pressure falloff behavior at the fuel loadings of the burning velocity measurements. Empirically, we found that applying a slightly less than linear pressure dependence to CH_2F_2 decomposition gave rate expressions providing a good fit to our burning velocity data at (1 bar, T_u=298 K), (2 bar, T_u=350 K), and (3 bar, T_u=400 K).

With these empirical rate expressions in hand, we then developed a supporting RRKM/Master Equation model implemented in ChemRate [56]. We utilized an *ab initio* (G3B3) [55] transition state and a computed 0 K barrier of 327 kJ mol^{-1}. For energy transfer, in argon we used an exponential-

down model parameter of α = 0.85*T $cm^{-1} K^{-1}$, which yields a rate expression at 1 bar and (1200 to 1800) K with A = 1.35x10^{11} cm^3 mol^{-1} s^{-1} and E_a = 257.9 kJ mol^{-1}. Argon is not used in our experiments, however, and the primary bath gases in the pre-flame region where burning velocities are determined are O_2, N_2, and CH_2F_2. Relative to a value of 0.6 for argon, O_2 and N_2 have collision efficiencies of 1.0, [97] while that for CH_2F_2 is expected to be higher, with an estimated lower limit of about 2 and a maximum of about 6 based on the flame modeling work of L'Esperance et al. [37]. Using mole fraction weighed collision efficiencies, we computed effective rate expressions for the different conditions (P, T, ϕ) of our experiments, and utilized them in our burning velocity models. In these computations, we then varied the collision efficiency for CH_2F_2 and found that a value of 2.0 (relative to nitrogen) gave the best agreement with experiment. We initially used a relative CH_2F_2 collision efficiency of 6.0 from L'Esperance et al. [37], but found this produced burning velocities that were far too high at high pressures (3 bar) and large O_2 loadings (30 to 40) %.

As discussed in detail in the paper describing our burning velocity measurements,[8] our optimization procedure has added uncertainty because derived burning velocities depend on the burning velocity model used to simulate the experiments, wherein energy-loss assumptions in the burned gas can range from adiabatic (no heat lost from radiation) to optically-thin (all thermal radiation lost) and this results in differences of (10 to 15) % in the derived burning velocity. Nonetheless, our final optimized RRKM model for CH_2F_2 decomposition is in very good agreement with the subsequently published data and model of Matsugi and Shiina. [94] Our rate constants in the range (1800 to 2100) K agree within about ± 20 % with the data of Matsugi and Shiina – this includes both rate constants from our RRKM/Master Equation modeling and those that provide best fits to our burning velocities.

Our RRKM/Master Equation model allows the calculation of rate constants for discrete conditions, but for detailed kinetics models it is necessary to parameterize the results in a concise form describing a wide range of conditions. For this purpose, we used the Troe formulation of the pressure and temperature dependent rate expression, $k = k_\infty (P_r/(1+P_r)) F(P_r)$, where $P_r = k_0[M]/k_\infty$ is a reduced pressure, [M] is the third-body efficiency weighted concentration of the mixture, k_∞ is the

high-pressure limit, k_0 is the low-pressure limit, and $F(P_r)$ is a function determined by a Troe broadening factor of F_c. [95] We used the Troe form for $F(P_r)$ and found a good fit to our data using F_c=0.08. Because the Troe formulation cannot reproduce all subtleties of the RRKM model, adjustments were made within uncertainty limits to the high-pressure k_∞ and low-pressure k_0 limits to arrive at a parameterization that best fit available data and described results over the conditions of interest. The final values are given in a list the end of this paper. We estimate the uncertainty factor for this rate constant to be about f=1.6 (in our range of interest (1 to 3) bar and (1200 to 1800) K) from the range of values used in our fits to the data in our flame modeling, and comparison with our RKKM/Master equation rate constants, and comparison to the recent measurements by Matsugi and Shiina.

In conjunction with the rest of our kinetics model, we find good agreement (3% to 6%) between measured and computed burning velocities over a wide range of conditions: oxygen mixture fractions of (21 to 40) %, pressures of (1 to 3) bar, and equivalence ratios of (0.8 to 1.3).

$CH_2F_2 + X \rightarrow CHF_2 + HX$ (X = H, O, OH, F)

The rate expressions for these reactions, we have taken from our recent work for H abstractions from the fluoromethanes.[7] The individual reactions are discussed briefly below – for a more detailed analysis see the cited paper, including figures comparing the recommended rate constants with the data reported in the literature. Only the $CH_2F_2 + H \rightarrow CHF_2 + H_2$ reaction has a discernable impact on burning velocities. In addition, the reaction with OH is important for reactions involving recycling H, O, and OH in the pre-flame radical initiation phase (but does not impact burning velocities). All of these reactions, however, are important to the destruction of CH_2F_2 in the combustion flame zone.

$CH_2F_2 + H \rightarrow CHF_2 + H_2$

The rate expression for this reaction we have taken from our recent work for H abstractions from the fluoromethanes by the flame radicals H, O, OH, and F. [7] There have been no direct measurements of the rate of reaction for $CH_2F_2 + H \rightarrow CHF_2 + H_2$, although there has been a single measurement of this reaction in the reverse direction $CHF_2 + H_2 \rightarrow CH_2F_2 + H$ over a limited temperature range (500 to 635) K by Pritchard and Perona. [98] We estimated the rate of reaction over a wide temperature range considering the measurements by Pritchard and Perona and several additional sources of information: the experimental results (605 to 871) K of Westenberg and DeHass[99] for the homologous reaction $CH_3F + H \rightarrow CH_2F + H_2$ and the relative rates for $CH_3F + H$ and $CH_2F_2 + H$ as derived from the quantum and transition state theory results of Matsugi and Shiina. [100] Based on the uncertainties in the experimental data, and estimated uncertainties in our parametric fits, we estimate the uncertainty in the rate constant to be a factor of f=1.6 at (1200 to 1800) K. During flame model optimization we also varied rates for $CH_2F_2 + H$, but found that "optimized" values produced burning velocities with uncertainties that were statistically similar to the unmodified rate expression, which we ultimately adopted. Our analysis says this reaction has a small, but observable impact on flame velocities (see above in Section 2, where values for the dependence of burning velocities on rate constants are provided along with a discussion).

$CH_2F_2 + O \rightarrow CHF_2 + OH$

The rate expression for this reaction we have taken from our recent work for H abstractions from the fluoromethanes by the flame radicals H, O, OH, and F. [7] There are no measurements on the rate of reaction for $CH_2F_2 + O \rightarrow CHF_2 + OH$. As discussed in our H abstraction paper,[7] in order to estimate the rate of H abstraction from CH_2F_2 by O atoms, we made use of experimental data from the homologous reaction $CH_3F + O \rightarrow CH_2F + OH$ from the shock tube measurements at (920 to 1570) K by Miyoshi et al. [101] and coupled these with relative rates at high temperatures for both CH_3F and CH_3F_3 from the quantum chemical calculations and transition state theory work of Matsugi and Shiina [100] to achieve a self-consistent estimate valid for a wide temperature range. Based on the uncertainties in the rate constants for the reference reaction and the uncertainties in the parameterization of the rate expression, we estimate an uncertainty factor of about f=1.4 in the

absolute rate of this reaction. During flame model optimization, we also varied the rates of reaction, but found that this reaction had little impact on flame velocities.

$CH_2F_2 + OH \rightarrow CHF_2 + H_2O$

The rate expression for this reaction we have taken from our recent work for H abstractions from the fluoromethanes by the flame radicals H, O, OH, and F. [7] Many workers have measured the rate of reaction $CH_2F_2 + OH \rightarrow CHF_2 + H_2O$ at low temperatures (200 to 500) K because of this reaction's importance in atmospheric chemistry. There are no measurements, however, at high temperatures relevant to combustion. For this reaction, we utilized the recommended rate expression at low temperatures (220 to 380) K from the NASA/JPL evaluation by Burkholder et al. [102]. In order to predict rate constants over a wide temperature range, we made use of the reference homologous reaction $CHF_3 + OH \rightarrow CF_3 + H_2O$, where there are rate constant measurements at both high (1000 to 1700) K and low (300 to 500) K temperatures. We also made use of relative rate constants at high temperatures for these two reactions based on the quantum chemical calculations of Matsugi and Shiina [100]. Based on trends in the other fluoromethanes + OH, we estimated the curvature in the rate expression, mainly due to tunneling, and determined a "best" fit for the temperature exponent (T^n). Based on the uncertainties in the experimental data and the uncertainty in the parameterization, we estimate an uncertainty factor of about f=1.5 at high temperatures. As with other reactions in this homologous series $CH_2F_2 + X$, during flame model optimization, we varied the rates of reaction for this class of reaction, but they had little impact on flame velocities ($CH_2F_2 + H \rightarrow CHF_2 + H_2$ had a slight discernable impact).

$CH_2F_2 + F \rightarrow CHF_2 + HF$

The rate expression for this reaction we have taken from our recent work for H abstractions from the fluoromethanes by the flame radicals H, O, OH, and F. [7] There is a reliable measurement of $CH_2F_2 + F \rightarrow CHF_2 + HF$ at low temperatures (180 to 300) K by Persky. [103] We extended this to higher temperatures using an extended Arrhenius expression with n=1.44; this was the "best"

parameterized value based on the trends in this parameter for the other fluoromethanes. For the other fluoromethanes (including methane), there are no measurements for H abstraction by F atoms above about 500 K. There are several quantum chemical calculations reported in the literature for these reactions (see for example, Wang et al. [104]). We did not use the functional forms for the rate constants from those works. We estimate an uncertainty factor of f=1.4 for the rate constants based on the uncertainty in the temperature exponent. During flame model optimization we also varied the rates of reaction, but found that this reaction had little impact on flame velocities.

Fluorinated Hydrocarbons: CHF_2

$CHF_2 + O_2 \rightarrow CF_2O + OH$

This reaction is exothermic by about 326 kJ mol^{-1}. The pre-exponential A factor in the rate expression was estimated by analogy to that for $CH_3 + O_2 \rightarrow CH_2O + OH$ from the 2005 work of Srinivasan et al. [105], correcting for reaction path degeneracy (1/3), using a temperature dependence (T^n) of n=1, and assuming no barrier since this reaction is highly exothermic and is a radical-radical and concerted reaction. In this reaction, the CHF_2 adds to the biradical O_2, then there is an internal rearrangement where the H atom is transferred to the ROO* radical site (becoming *QOOH), which then immediately decomposes by beta scission of OH. Our flame modeling where we included this reaction in our optimizations suggested a weak temperature dependence on the order of (5 to 15) kJ mol^{-1} ($k \propto e^{-E/RT}$), or roughly equivalent to the T^{-1} dependence. This reaction has small promoting effect on burning velocities and very weakly impacts the dependence of burning velocities on equivalence ratio and pressure. Nevertheless, it is an important pathway in the pre-flame processes and contributes to chain propagation. In our optimizations, we varied this rate constant by factors of 2 to 8 (variously changing both A and E), and found a range of values that gave statistically similar fits. We ultimately selected an intermediate rate expression and have estimated an uncertainty factor of f=1.8. For this rate expression, the A factor and E are about 2.5 and 2.8 times lower than those for the rate expression for $CH_3 + O_2 \rightarrow CH_2O + OH$ from Srinivasan et al, and at (1200 to 1800 K), and the overall rate constants are about (2.5 to 6) times faster. The possible pathways $CHF_2 + O_2 \rightarrow CHF_2O + O$ and $CHF_2 + O_2 \rightarrow CF_2O + O + H$ are energetically far less favorable than the $CF_2O + OH$ channel and therefore are not competitive, nor included in the mechanism.

$CHF_2 + H \rightarrow CHF + HF$

This reaction is exothermic by about 100 kJ mol^{-1}. The kinetics were estimated by analogy to $CF_3 + H \rightarrow CF_2 + HF$, for which Takahashi et al. [106] determined a rate constant of $(5.3\pm0.2)x10^{13}$ cm^3 mol^{-1} s^{-1} at 1150 K to 1380 K, independent of temperature and pressure. That work used the simultaneous shock-induced thermal decompositions of CF_3I and C_2H_5I to create CF_3 and H, respectively, in dilute argon and then derived rate constants on the basis of H atom decay rates monitored with atomic resonance absorption spectroscopy (ARAS). They also carried out *ab initio* and multi-channel RRKM calculations[57] to investigate possible product channels. The reaction was found to be a fast radical combination followed by a chemically activated 1,1-HF elimination. For the analogous $CHF_2 + H$ case of current interest, we increased the *A* factor slightly to provide an upper limit of $6.5x10^{13}$ cm^3 mol^{-1} s^{-1} to reflect the ease of forming CHF compared to CF_2 (low vs high lying triplet states, respectively). Although this reaction is a contributing pathway for destruction of CHF_2, it is not a rate determining step and its exact value was found to have little impact on computed burning velocities.

$CHF_2 + O \rightarrow CF_2O + H$

No rate measurements for this reaction appear to exist. The reaction is exothermic by about 394 kJ mol^{-1} and involves the formation of an unstable difluoromethoxy intermediate. A rate constant was estimated on the basis of the 1998 Takahashi et al. [106] shock tube study of the analogous process $CF_3 + O \rightarrow CF_2O + F$. In that work, they thermally decomposed dilute mixtures of CF_3I and nitrous oxide in argon to create CF_3 and ground state O atoms, respectively, and then monitored the decay rate of O with atomic resonance absorption spectroscopy (ARAS) in order to determine the kinetics. They found a rate constant of $(1.54\pm0.14)x10^{13}$ cm^3 mol^{-1} s^{-1} at (1900 to 2300) K independent of temperature and pressure. *Ab initio* and RRKM calculations were used to investigate and confirm the product channel. The reactions of O with CF_3 and CHF_2 both involve fast radical combinations to form an activated fluoromethoxy species, followed by a beta scission of H atoms. However, in contrast to $CF_3 + O$, where available channels are reversal or fission of the C–F bond, the $CHF_2 + O$ system is expected to be dominated by fission of the weak C–H bond, a process about 85 kJ mol^{-1} more exothermic than reactions available to $CF_3 + O$. The expected dominance of the $CF_2O + H$ channel is consistent with *ab initio* studies of the analogous fluoromethoxy system[107]. Compared with $CF_3 + O$, we increased the A factor slightly to account for thermochemical differences, the

weaker C–H bond, lighter H atom, and that the reference reaction CF_3 + O likely constitutes a lower bound. Given these considerations we estimated the rate constant as $3.7x10^{13}$ cm^3 mol^{-1} s^{-1}. This results in relative rate constants for CF_3 and CHF_2 that are similar to the ratio of rate constants observed for the reactions CCl_3 + O and $CHCl_2$ + O by Slagle and coworkers [108, 109]. Although CHF_2 + O is a major destruction pathway for CHF_2, it is not a rate determining step in this combustion pathway and the rate constants have little impact on computed burning velocities. We estimate an uncertainty factor of *f*=2..

$CHF_2 + OH \rightarrow CHFO + HF$

This reaction is a radical combination, followed by a facile 1,2-elimination of HF. It is highly exothermic (about 449 kJ mol^{-1}) and is expected to be a pressure-independent direct process under typical combustion conditions. In prior mechanisms for the destruction of fluorinated hydrocarbons [44], rate constants for this and analogous fluoromethyl reactions were estimated with upper limit values of (2 to 5)$x10^{13}$ cm^{-3} mol^{-1} s^{-1}. More recently, Srinivasan et al. in 2007[110] measured the rate constant of the analogous reaction $CF_3 + OH \rightarrow COF_2 + HF$ in a shock tube at high temperatures (1300 to 1700) K at about $1.0x10^{13}$ mol cm^{-3} s^{-1}. In our modeling of the R-32 flame and for other refrigerants, we found a slightly higher value (x2.4) was a “best” fit value. We then increased this by a factor of 2 to provide an upper limit. Although this reaction contributes to the destruction of CHF_2, the rate constant is large and the rate determining step of this combustion path is formation of CHF_2, not its subsequent reactions. Consequently, in a combusting system, CHF_2 is rapidly destroyed and is present only at small, near steady-state concentrations. Small changes in its destruction rate, thus only slightly change the concentration of CHF_2 and have little impact on the overall combustion rate.

$CHF_2 + HO_2 \rightarrow CH_2F_2 + O_2$

This reaction is a radical disproportionation where the radical CHF_2 abstracts the hydrogen beta to the radical site in HO_2. We estimated the rate expression by analogy to that for $CH_3 + HO_2 \rightarrow CH_4 + O_2$ from the work of Jasper et al. ,[111] where we have increased the barrier by 6.5 kJ mol^{-1} to account for the lower exothermicity for this reaction. The contribution of this reaction to the reaction flux is small, but is included for completeness in the mechanism.

$CHF_2 + F \rightarrow CF_2 + HF$

This reaction is a radical combination followed by a 1,1-HF elimination and is exothermic by about 303 kJ mol^{-1}. Although unmeasured to our knowledge, one expects under combustion conditions a direct pressure-independent process with a large rate constant with no barrier typical for a radical recombination (especially since F atoms are highly reactive). We provide an upper limit estimate of $3.0x10^{13}$ cm^{-3} mol^{-1} s^{-1} using $CHF_2 + H \rightarrow CHF + HF$ as a reference reaction (see discussion for that reaction), but we reduced the rate constant by about a factor of 2 to account for the heavier F atom. Using this rate constant, this reaction is a very minor destruction pathway for CHF_2.

$CHF_2 + CHF_2 \rightarrow CHFCF_2 + HF$

This reaction is exothermic by about 284 kJ mol^{-1}. The rate expression is based on the *ab initio* transition state and RRKM calculations of Burgess et al. [44] We increased the rate constants from that work by about 1.4 to provide an upper limit where the contribution from this reaction had a relatively small, but discernable impact. This reaction is responsible for the formation of the fluoroethylene $CHFCF_2$ which is created during the pre-flame phase and then is destroyed during the combustion phase through reactions with O atoms forming CHFO, CF_2O, and CFO. This reaction has a small impact on burning velocities and only weakly impacts the dependence of burning velocities on equivalence ratio and pressure. Nevertheless, it is the primary pathway for the destruction of CHF_2 in the pre-flame phase.

$CHFCF_2 + O \rightarrow$ Products

Cvetanovic in 1987 evaluated the reactions of O atoms with unsaturated hydrocarbons, including the fluoroethenes. [112] On the average for the halogenated ethenes, the rate expressions (with unspecified products) over the range (300 to 500) K could be described with about $A = 5x10^{12}$ mol cm^{-3} s^{-1} and $E = 8$ kJ mol^{-1} with an uncertainty factor f for A of about 2 and an uncertainty in E of about 1 kJ mol^{-1}. Specifically, for $CHFCF_2 + O \rightarrow$ *Products*, Cvetanovic recommended a rate expression with $A = 6.1x10^{12}$ mol cm^{-3} s^{-1} and $E = 7.9$ kJ mol^{-1}. His recommended rate expression was largely based on the relative rates for the fluoroethenes measured by Jones and Moss in 1974.[113] Umemoto et al. in 1985 reported a rate expression for this reaction with $A = 3x10^{12}$ mol cm^{-3} s^{-1} and $E = 4.5$ kJ mol^{-1}.[114] The barriers reported by Umemoto et al. for this and other fluoroethene reactions are somewhat lower than those reported by others: about 5 kJ mol^{-1} versus 8 kJ mol^{-1}. Although the rate constants from both of these works are very close at 500 K, at 300 K the value of Umemoto et al. is almost twice as fast. Other workers have determined rate constants for this reaction near room temperature with the value by Gilbert et al. [115] about 30 % faster than that from Umemoto et al. and the value from Lee et al. in 1996 [116] is about the same as that recommended by Cvetanovic. Our interest here is providing an upper limit for this reaction. Although we found the rate constants used here had no impact on burning velocities, they were important pathways for destruction of $CHFCF_2$. We fit the low temperature rate constants of Umemoto et al. with an estimated temperature exponent of $n = 1.3$ in order to extend the rate constants to flame temperatures. We increased the A factor by about 2.5 to provide an upper limit and then estimated branching ratios of (1.0, 0.8, 0.6) for the 3 possible channels $CHFCF_2 + O \rightarrow$ ($CHFO + CF_2$, $CFO + CHF_2$, $CF_2O + CHF$).

Fluorinated Hydrocarbons: CHF

$CHF + O_2 \rightarrow CHFO + O$

This is a key reaction affecting computed burning velocities in the combustion of CH_2F_2. It is found to influence the relative burning velocities under rich versus lean conditions. The reaction initiates pre-

flame processes for radical chain propagation through the generation of O atom radicals from the reactant O_2. The CHFO product quickly decomposes to CO and HF products, thus eventually releasing heat upon formation of CO_2 and increasing the system temperature.

$CHF + O_2 \rightarrow CHFO + O$ is exothermic by about 282 kJ mol^{-1}. There appears to be no experimental measurement of the rate constant. However, Keating and Matula [117] carried out a shock tube investigation of the analogous reaction $CF_2 + O_2 \rightarrow CF_2O + O$ and determined for that process an activation energy of about 110 kJ mol^{-1} (suggesting a 0 K barrier on the order of about 90 kJ mol^{-1}). The reaction involves partially breaking the paired electrons in the ground (singlet) state of CF_2 and involves formation of a short-lived intermediate peroxy biradical (i.e., $\bullet CF_2OO\bullet$). Consequently, in analogous molecules the barrier should scale with the triplet-singlet separation. The triplet state of CF_2 is about 237 kJ mol^{-1} above the singlet ground state based on the high-resolution measurements of Zhou et al. [118]. Thus, the activation energy for this reaction is about 46 % of the triplet energy. Applying this same percentage to the triplet energy of CHF (62 kJ mol^{-1} from the measurements of Murray et al, [119]) yields an estimated activation energy for the analogous reaction of $CHF + O_2 \rightarrow CHFO + O$ of about 29 kJ mol^{-1}. This derived barrier for reaction of O_2 with CHF being lower than that for CF_2 is consistent with the greater exothermicity of the former process, which is more favorable by about 119 kJ mol^{-1}. Our *a priori* estimate for the rate expression used an *A* factor from the CF_2 reaction with our estimated activation energy. In our flame modeling, we found that reasonable agreements with the experimental burning velocities could be obtained using activation energies that ranged (15 to 45) kJ mol^{-1}. Our "optimized" value of 32.6 kJ mol^{-1} best represented the relative burning velocities at high and low equivalence ratios. We note that larger rate constants for this reaction increased burning velocities to a greater degree at high equivalence ratios than at low equivalence ratios.

In our modeling of the CH_2F_2 flame, the *A* factor for this reaction $CHF + O_2 \rightarrow CHFO + O$ was adjusted within uncertainty limits to best agree with the experimentally-derived burning velocities. This was done iteratively in conjunction with the rate expression for $CH_2F_2 \rightarrow CHF + HF$. The burning velocities as a function of equivalence ratio are very sensitive to the rate of this reaction – and

consequently, the magnitude of this reaction is important to reproduce burning velocities at different conditions.

$CHF + H_2O \rightarrow CH_2O + HF$

This process is exothermic by about 288 kJ mol^{-1} and is a possible destruction pathway for CHF. The reaction forms CH_2O, which relatively quickly leads to the formation of HCO [through the reactions $CH_2O + X \rightarrow HCO + HX$ (X = H, O, OH)], and then to the formation of HO_2 (via $HCO + O_2 \rightarrow CO + HO_2$), which is an important species during pre-flame processes. Our rate expression is from the ab initio transition state and RRKM calculations of Zachariah et al. [53] and has a relatively small activation energy of about 27 kJ mol^{-1} at combustion-relevant temperatures, suggesting a 0 K barrier of about (10 to 15) kJ mol^{-1}. Under our conditions, the rate constant has no significant impact on computed burning velocities, but is included in the mechanism for completeness.

$CHF + H \rightarrow CH + HF$

$CHF + H \rightarrow CF + H2$

These processes are moderately exothermic (by 43 kJ mol^{-1} and 120 kJ mol^{-1}, respectively) and the rate expressions are based on the room temperature measurements of Tsai and McFadden. [120]. One expects the rate constants to exhibit little dependence on temperature. We assigned the product channels as 2 to 1 for CH + HF versus CF + H_2. The reactions proceed via combination followed by 1,1 eliminations of H_2 or HF. Although the H_2 formation channel is more exothermic by about 77 kJ mol^{-1}, it lacks a favorable ionic component, making the HF elimination channel likely to be favored (as with closed-shell fluoromethanes). These reactions have little impact on our computed burning velocities, because they occur in the combustion phase and are not rate-determining steps in the overall oxidation. Nevertheless, they need to be included to complete reaction pathways to products.

CHF + O ⟶ CO + HF

The large exothermicity of about 780 kJ mol^{-1} should make this a direct process under typical combustion condition with no formation of a stable intermediate and no pressure dependence in the rate. Our rate constant is from the room temperature measurements of Tsai and McFadden [120], and likely has only a small temperature dependence since the rate constant is very high at low temperatures (it is essentially a radical-radical reaction – CHF, a carbene, has a very reactive lone pair). It is very fast and not a rate determining step, however, so its exact value has little effect on modeled burning velocities.

CHF + OH ⟶ CHFO + H

CHF + OH ⟶ HCO + HF

The first reaction channel forming CHFO + H reaction is exothermic by about 350 kJ mol^{-1} and under typical combustion conditions is expected to be a direct process with no stabilized intermediate. No measured values appear to exist. As a reference reaction, we consider the analogous reaction CF_2 + OH ⟶ CF_2O + H, which was measured by Srinivasan et al. [121] at high temperatures and pressures in a shock tube. They determined the rate constant of CF_2 + OH to be independent of temperature within their uncertainties, finding a value of (9.64±0.36)x10^{12} cm^3 mol^{-1} s^{-1} at (1800 to 2200) K. They used transition state theory to predict a small activation energy of about 8 kJ mol^{-1} at combustion temperatures. For CHF + OH ⟶ CHFO + H, we estimate a rate constant 2x10^{13} cm^3 mol^{-1} s^{-1} – a factor of two faster than that for CF_2 + OH, since CHF is a more reactive species. Using this increased rate constant, this reaction CHF + OH is still a minor channel for the destruction of CHF. For the second reaction channel forming HCO + HF, we utilized the estimated rate constant from the flame studies of Biordi et al. [122] This also is a very minor channel for destruction of CHF.

$CHF + CHF \rightarrow C_2HF + HF$

This combination/elimination reaction is exothermic by about 464 kJ mol^{-1} and no stabilization of the intermediate is expected under typical combustion conditions. The rate expression is derived from that given in earlier work [44], but was increased by about a factor of 5 to provide an estimated upper limit, at which point it had only a very slight impact on burning velocities.

$CH_2F_2 + CHF \rightarrow CHFCHF[Z] + HF$

We are unaware of any experimental studies of this reaction, which is exothermic by about (280 to 320) kJ mol^{-1}. One expects it to proceed via an insertion/elimination mechanism. Although there are three similar product channels that eliminate HF – with formation of CH_2CF_2, CHFCHF[*E*], and CHFCHF[*Z*], we have only included this one channel as a surrogate for all of the channels.

Cobos et al. in 2017 [123] using a computed *ab initio* transition state report energetics and a rate expression at (1800 to 2200) K for another channel $CH_2F_2 + CHF \rightarrow CHF_2 + CH_2F$ which is an insertion to form an activated fluoroethane CHF_2-CH_2F followed by C-C bond fission. In that work, they measured the change in density of a number of species in a shock tube at high temperatures (1800 to 2200) K and estimated/calculated rate constants for a number of reactions from their kinetic modeling and of the decomposition of CH_2F_2. This alternate reaction channel $CHF_2 + CH_2F$ is endothermic by about 32 kJ mol^{-1} with a computed barrier of about 51 kJ mol^{-1} – that is, the reverse reaction has a barrier of about 20 kJ mol^{-1}. Cobos et al. did not include the insertion/elimination channel $CH_2F_2 + CHF \rightarrow CHFCHF[Z] + HF$ which we believe should be important. Matsugi and Shiina in 2018 [94] used *ab initio* calculations to compute the barrier to insertion of CHF into CH_2F_2 and found it to be about 50 kJ mol^{-1}. They computed a total rate expression (at the high pressure limit) for the three reaction channels: CH_2CF_2, CHFCHF[*E*], and CHFCHF[*Z*] products. They did not include the C-C bond fission channel likely because it is an endothermic reaction, while the HF elimination channels are highly exothermic.

This reaction does not affect modeled burning velocities when using an estimated upper-limit rate constant. This reaction, however, is necessary to complete the reaction pathways to final products. In 1995, we computed rate expressions (at 1 bar) for these type of reactions using *ab initio* transition states and RKKM calculations.[44] In the mechanism reported here, we provide what we consider an upper-limit rate constant where we have increased the *A* factor for the Matsugi and Shiina rate expression by about a factor of 2. Note this is about 4 times slower than that of Burgess et al. [44] and about 7 times faster than that for the C-C bond fission channel $CH_2F_2 + CHF \rightarrow CHF_2 + CH_2F$ from the work of Cobos et al..

$CHFCHF[Z] + O \rightarrow CFO + CH_2F$

We fit the rate expression for this reaction over the range (300 to 500) K as recommended by Cvetanovic [112] using a temperature exponent of n = 1.0 to extended the rate constants to flame temperatures. This reaction has no impact on burning velocities, but is an necessary pathway for destruction of CHFCHF[*Z*].

Fluorinated Hydrocarbons: CF_2

$CF_2 + O_2 \rightarrow CF_2O + O$

This reaction is a secondary pathway for the destruction of CF_2 and is exothermic by about 163 kJ mol^{-1}. In shock tube studies at (1670 to 2500) K and (4 to 7) bar, Keating and Matula[117] determined rate constants for $CF_2 + O_2 \rightarrow CF_2O + O$ by thermally decomposing C_2F_4 to $2CF_2$ in the presence of O_2 and following the formation rate of CF_2O with infrared emission and CF_2 concentrations with ultraviolet absorption spectroscopy. Their conditions were similar to the flame conditions of current interest. We extended their reported rate constants to lower temperatures by assuming a modified Arrhenius format with a temperature exponent (T^n) of n=1.5. We then utilized a simple Arrhenius fit at high temperatures (1500 to 1800) K with an *A* factor slightly reduced by 1.24

through our optimization of the rate expression in this model (and our work on other fluorinated hydrocarbons, not reported here).

$CF_2 + H_2O \rightarrow CHFO + HF$

This reaction is exothermic by about 219 kJ mol^{-1}. Our rate expression is from the *ab initio* transition state and RRKM calculations of Burgess et al. [44] The process makes only a very minor contribution to the destruction of CF_2 and has no significant impact on the calculated burning velocities.

$CF_2 + H \rightarrow CF + HF$

This reaction is about 50 kJ mol^{-1} exothermic. Biordi et al. in 1976[124] reported an estimated rate constant of (1.0 to 2.4)x10^{13} cm^3 mol^{-1} s^{-1} for CF_2 + H at 1800 K based on mass spectrometric studies of methane-oxygen-argon flames inhibited with CF_3Br. In more-direct shock-tube experiments that we prefer, Yamamori et al. in 1999 [125] determined the rate constant to be about a factor of 2 times slower than Biordi et al. and found it to be independent of pressure with a slight temperature dependence (E_a ~ 20 kJ mol^{-1}) at 1450 K to 1850 K. Yamamori et al. simultaneously generated H and CF_2 from the respective decompositions C_2H_5I and $CHClF_2$ and determined the rate constant from the H atom decay profiles monitored with ARAS. They also carried out *ab initio* calculations at the G2 level of theory, finding the channel to CF + HF to be far lower in energy than other possibilities. At room temperature, there is measurement of CF_2 + H in a plasma by Ryan and Plumb reported in 1984[126] that is qualitatively consistent with the high temperature results.

There is another room temperature measurement by Tsai and McFadden[127] which is about a factor of 200 higher than the value of Ryan and Plumb – and even about 2.5 times that of the high temperature measurements of Yamamori et al. Relatively recently, Cobos et al. in 2017 reported a rate expression for this reaction at high temperatures (1800 to 2200) K from their kinetic modeling

of the decomposition of CH_2F_2.[123] Their rate constants are about a factor of 5 lower than the high quality direct measurements of Yamamori et al, a factor of 10 lower at 1000 K, and when extended to room temperature about a factor of 500 lower than the measurements of Ryan and Plumb. In addition, their effective activation energy at combustion temperatures is about 45 kJ mol^{-1} – much higher than it should be for addition of H atom to a carbene, lone pair, or alkene – which should be only on the order of (5 to 15) kJ mol^{-1}. We disregard the reported experimental rate constants of Tsai and McFadden and the indirect modeled rate constants of Cobos et al. in favor of the high quality direct measurements of Yamamori et al.

In Table 2, we provide a modified Arrhenius expression using a temperature exponent (T^n) of n=1.0 that agrees with both Yamamori et al. and Ryan and Plumb to within a few percent. We utilized in the kinetics model a two-parameter Arrhenius fit (also provided in the table) specific to the temperature range (1600 to 2100) K relevant to the combustion of CH_2F_2. This reaction is a very minor channel and very nearly at equilibrium – and thus needs to be included in the mechanism. From the range of the Biordi et al. and Yamamori et al. measurements, we estimate an uncertainty factor of f=2 at flame temperatures.

$CF_2 + O \rightarrow CFO + F$

This reaction is about 151 kJ mol^{-1} exothermic on the ground state surface. An approximate temperature-independent rate constant of (1 to 5)x10^{13} cm^3 mol^{-1} s^{-1} for CF_2 + O at 1800 K was estimated by Biordi et al. in 1976 from their mass spectrometric studies and kinetic modeling[124] from their mass spectrometric studies of methane-oxygen-argon flames inhibited with CF_3Br. More direct shock-tube experiments at (2017 to 2429) K by Yamamori et al. in 1999 [125] yielded a value of 2.45x10^{13} cm^3 mol^{-1} s^{-1} consistent with that of Biordi et al. The Yamamori et al. work utilized nitrous oxide and $CHClF_2$ as precursors of O atoms and CF_2, respectively, and the derived rate constants were based on O atom decay profiles. They also carried out G2-level *ab initio* calculations to confirm the product channel and that there was no barrier to addition. A number of workers have measured the rate of reaction CF_2 + O → *Products* at room temperature with values ranging

from (0.98 to 1.2)x10^{13} cm^3 mol^{-1} s^{-1} where they indicate the likely products were CFO + F.[128-131]. We utilized the rate constant of Yamamori et al. along with the room temperature measurements to determine a rate expression with no barrier and a weak T^n (n=0.4) temperature dependence (equivalent to about E_a = 2.3 kJ mol^{-1}). We estimate an uncertainty factor of about f=2. This is a secondary channel for the destruction of CF_2.

$CF_2 + OH \rightarrow CF_2O + H$

$CF_2 + OH \rightarrow CFO + HF$

Biordi et al. in 1976 [86] estimated the rate constant for $CF_2 + OH \rightarrow$ *Products* to be approximately (1 to 3)x10^{13} cm^3 mol^{-1} s^{-1} at 1800 K from mass spectrometric studies of species profiles in methane-oxygen-argon flames inhibited with CF_3Br. In later work in 1978 on the system with the same apparatus they derived a value of 5x10^{12} cm^3 mol^{-1} s^{-1} (1090 to 1375) K for the reaction $CF_2 + OH \rightarrow CF_2O + H$. [122] More direct measurements are the shock tube studies of Srinivasan et al. in 2008 [121], spanning 1800 K to 2200 K, who dissociated CF_3 in the presence of H_2O to create a system containing CF_2 and OH wherein the spectroscopically-monitored OH decay profiles were sensitive to rate constants for $CF_2 + OH \rightarrow CF_2O + H$. Their measured rate constant of (9.64±0.36)x10^{12} cm^3 mol^{-1} s^{-1} (1800 to 2200) K was only about 20 % smaller than their CASPT2 variable reaction coordinate transition state theory (VRC-TST) calculations that suggested an activation energy of about 6 kJ mol^{-1} at combustion temperatures. Srinivasan et al. concluded quite reasonably that the large exothermicity of the $CF_2O + H$ product channel (approximately 230 kJ mol^{-1} [121]) will preclude collisional stabilization under normal combustion conditions and that no pressure-dependence of the rate will be observed. Our flame model predicts $CF_2 + OH$ is the primary destruction pathway for CF_2 in R-32 flames, and our rate constants (Table 2) for the $CF_2O + H$ product channel are based on the data from Srinivasan et al. The CFO + HF product channel is more exothermic than $CF_2O + H$ by about 60 kJ mol^{-1}, but is expected to have a significantly larger reverse barrier, so the branching value is uncertain. In the absence of measurements, we have estimated a maximum value for the branching value based on Biordi et al. [124]. Computed burning velocities, however, were insensitive to changes in these rate constants.

Fluorinated Hydrocarbons: CF

$CF + O_2 \rightarrow CFO + O$

This reaction is the major loss pathway for CF, a short-lived steady-state species formed in R-32 flames primarily via $CHF + H \rightarrow CF + H_2$, a reaction that is only a secondary route for destruction of CHF. Consequently, CF is a minor intermediate in the presently modeled systems. The $CF + O_2$ reaction is about 174 kJ mol^{-1} exothermic. Rate constants have been measured in the temperature range of (258 to 780) K by Vetters et al,[132] following up an earlier room temperature study by the same group.[133] They generated ground state CF radicals via 2-photon photodissociation of CF_2Br_2 in helium mixtures containing O_2 as reactant and CF_4 as an efficient quencher of excited CF. Rate constants were determined by monitoring CF decay rates with laser-induced-fluorescence. Because the reaction $CF + O_2$ is fast and not a rate determining step in this oxidation path, the exact value is unimportant under our conditions. The process is needed, however, to complete the conversion of intermediates to final combustion products. Vetters et al. represented their data with a two-term Arrhenius expression, but rate constants can be adequately represented at combustion temperatures using only the high temperature term (errors in *k* of < 8 % above 1000 K) as given in Table 2.

$CF + O \rightarrow CO + F$

The reaction $CF + O \rightarrow CO + F$ is about 527 kJ mol^{-1} exothermic and is presumed to involve a radical combination with no stabilization of the intermediate. van Hoeymissen et al. in 1994 [134] measured the rate constant at room temperature using laser photodissociation/laser-induced fluorescence techniques (LPD/LIF). CF radicals were generated by photolysis of CF_2Br_2 and reacted with O atoms produced in a discharge-flow apparatus. From real-time CF decays monitored with LIF, the rate constant was determined as $(2.83\pm0.48)\times10^{13}$ cm^3 mol^{-1} s^{-1}, about a factor of three larger than the measurement of Tsai and McFadden reported in 1990 [130] in a discharge-flow apparatus utilizing photoionization detection of CF. The rate constant of van Hoeymissen et al. was obtained

under more dilute conditions likely better able to isolate the reaction and is more consistent with the relative rate measurements for CF + O and CF_2 + O by Booth et al. [135]. We have adopted their result and fit to a rate expression with A=8.0x10^{13}. This reaction is a minor channel for the destruction of CF, which primarily reacts with O_2 as discussed here elsewhere. The computed burning velocities were insensitive to the rate constant.

CF + OH → CO + HF

This reaction is about 667 kJ mol^{-1} exothermic and proceeds by a radical-radical combination to give an unstable intermediate that decomposes immediately under flame conditions. No measurements of the rate constant for CF + OH appear to exist. We estimated the value to be equal to that of CF + O → CO + F. This is another minor channel for the destruction of CF. The exact value employed very slightly affects the modeled near steady-state concentration of CF, but has no significant impact on computed burning velocities.

Oxygenated Hydrofluorocarbons: CF_2O, CHFO, CFO

CF_2O + H → CFO + HF

The rate expression(s) for this reaction were taken from the *ab initio* transition state and RRKM calculations of Zachariah et al. [54] [53]. This reaction proceeds through three separate elementary reaction pathways, involving addition of H to the carbon or the oxygen, followed by HF elimination, or via a direct abstraction channel. All of these pathways lead to the same products. The overall reaction is exothermic by about 60 kJ mol^{-1}. Three rate expressions, one for each distinct elementary reaction pathway, are provided in the kinetics model (labeled "DUP" in the Chemkin mechanism file). The overall rate constants used here agree well with the experimental rate constants reported by Biordi et al[136] and Richter et al. [137] For a further discussion of these reactions see the work by Zachariah et al.

CHFO + M ⟶ CO + HF + M

This 1,1 HF unimolecular elimination is approximately just 1 kJ mol^{-1} exothermic and is the predominate destruction pathway for CHFO under flame conditions, rapidly consuming the fluoroformaldehyde so that it is destroyed as fast as it is formed. Shock tube studies of the thermal decomposition were carried out by Saito et al. in 1984 [138] at temperatures of 1160 K to 1480 K. Emission spectroscopy was used to simultaneously monitor in real-time both loss of CHFO and formation of CO. The derived rate constants should be reliable. The reaction has also been explored theoretically by a number of researchers [139-146] and the barrier height has been established to be near 180 kJ mol^{-1}. The decomposition rate is pressure-dependent under flame conditions of typical interest and the rate expression used is from the RRKM fit by Burgess et al. [44] to the rate constants of Saito et al.

CHFO + H ⟶ CFO + H_2

The rate expression for this mildly exothermic reaction (approximately 12 kJ mol^{-1}) is estimated based on that for the analogous CH_2O + H reaction as given in the review of Tsang and Hampson [147]. With this rate constant, this reaction is a minor channel.

CHFO + O ⟶ CFO + OH

This reaction is exothermic by about 6 kJ mol^{-1} and the rate constant has been estimated by analogy to CH_2O + O measured by Klemm et al. [148] With this rate constant, this reaction is a minor channel.

CHFO + OH ⟶ CFO + H_2O

Wallington and Hurley provide an upper limit for this reaction at 295 K,[149] which is of little use at combustion temperatures, except via estimation and extrapolation. Instead, we have utilized the rate expression from the *ab initio* transition state calculations reported by Francisco in 1992.[150] The reaction is exothermic by about 73 kJ mol^{-1} and is a minor channel that should be considered for elimination in condensed versions of the mechanism. More recently, Wang and Li have performed higher level *ab initio* calculations and computed tunneling corrections to predict rate constants for this reaction.[151] Their rate constants are about an order of magnitude lower at combustion temperatures than those of Francisco. Since this is a minor channel and we consider the rate constants to be upper limits, and hence, we have utilized the rate expression of Francisco.

CFO + M ⟶ CO + F + M

C-F bond fission in CFO is endothermic by about 145 kJ mol^{-1}. To derive rate constants in conjunction with the thermochemistry, the rate expression for the reverse combination CO + F ⟶ CFO from Burgess et al. [44] has previously been employed directly and as later modified by Saso et al. [39], who increased the *A* factor by a factor of 3 to better fit experimental burning velocity measurements in CHF_3 doped flames. The present work uses a rate expression that is a combined fit to the room temperature measurement of CO + F + M (third order conditions) by Appleman and Clyne using a discharge-flow apparatus[152] and the directly measured decomposition rate of CFO in the low-pressure limit at (950 to 1050) K by Knyazev et al. [153] Knyazev et al. laser-photolyzed acetyl fluoride to generate CFO in a flow reactor and derived the kinetics by monitoring its decay rate with photoionization mass spectrometry. Our fit assumes a negative temperature coefficient[153] for the low pressure limit rate constant and used a temperature exponent (T^n) of n = -1.0. When extrapolated to combustion temperatures, this reduces the rate constant by a factor of 1.7 to 1.9 relative to a fit assuming Arrhenius behavior (i.e., n=0). The rate constant is nonetheless sufficiently large that the exact value had no discernable impact on our computed burning velocities. Reaction Rate Expressions

Reaction Rate Expressions

Table 2 summarizes the rate expressions used in this work. If a single value was selected from the literature, the relevant reference is given. If the recommended rate expression is based on our evaluation of multiple literature sources, it is denoted "this work eval" and a discussion of the evaluation can be found above under the corresponding reaction listing. In a few cases, the rate expressions are our upper-limit estimates made either by analogy to other reactions or based on calculations – these are denoted "this work est." Reactions so estimated were found to have little-to-no impact on burning velocities – they are not rate-determining and simply provide pathways to complete the combustion of immediate species. Since these are upper limit estimates and the present studies provide no significant information on the actual rate constants, one should be cautious in the use of these estimates in other situations. Finally, there are several rate expressions that were adjusted (within their uncertainty limits) to achieve best agreement between the experimentally-derived and model burning velocities – these are denoted "this work model." We have estimated uncertainty factors *f* for some of the most important reactions from our modeling. For the other reactions, it would be difficult to estimate uncertainty factors, although *f*=2 is generally a good estimate for fast reactions and *f*=(2 to 4) for other reactions.

Summary

In summary, in this work, we compiled, evaluated, calculated, and estimated rate expressions that describe the reaction pathways for the decomposition and combustion of CH_2F_2 in $CH_2F_2/O_2/N_2$ flames. A chemical kinetic mechanism was constructed and used (in other work) [8] to model freely-propagating premixed flames and predict burning velocities which were compared to experimentally-derived burning velocities over a wide range of conditions (oxygen loadings, pressure, initial temperature, equivalence ratios). In that work, the agreement between modeled and experimental burning velocities was good (3 % to 6 %) and provides a validation of the chemical kinetic mechanism presented here.

Acknowledgments

This work was partially supported by the Building Technologies Office of the U.S. Department of Energy, Office of Energy Efficiency and Renewable Energy under contract #DE-EE-0007615 with Antonio Bouza serving as Project Manager.

Supporting Information

Supporting information gives the Chemkin-format kinetics model as optimized elsewhere [8]

to experimental burning velocities. Reactions, rate parameters, NASA format thermodynamic polynomials, and transport properties are included.

Author Declarations

The authors have no conflicts to disclose.

Data Availability

The data that supports the findings of this study are available within the article and its supplementary material.

Appendix: Species and Reaction Identifiers

In Table A1, for each species in this mechanism containing fluorinated hydrocarbon (C/H/F), and oxygen-containing fluorinated hydrocarbon (C/H/F/O) species, we provide several identifiers: InChI, Chemical Abstracts Registry Numbers (CASRN), and NIH PubChem Compound Identifiers (PubChem CID).

We also provide InChI-ER identifiers for each of the reactions in this mechanism containing hydrogen/fluorine (H/F), hydrogen/oxygen/fluorine species (H/O/F), fluorinated hydrocarbon (C/H/F). and oxygen-containing fluorinated hydrocarbon (C/H/F/O) species. InChI identifiers are widely used to provide structural/connectivity information for molecular species. InChI identifiers are unique representations. Each structure generates a unique InChI, and conversely each InChI generates a unique structure. [154] [155] [156].

In a similar fashion, InChI-ER identifiers are extensions of base InChI identifiers and are used to provide structural and chemical information for elementary reactions.[157-159] Like InChI, InChI-ER

has many layers that provide different types of (orthogonal) information about the elementary reactions. Each layer is proceeded by a slash followed by a character, i.e. "/v" "/c" "/h". Within each layer individual contributions are delimited by semicolons. The layers are described in Table A2.

Standard Hill-sorted notation is used to denote the molecular formula and the numbering follows this ordering except H atom are numbered last. For example, the molecular formula for formyl fluoride is CHFO with the C labeled #1, F as #2, O as #3, and lastly H as #4. The H atoms are not included in the molecular connectivity layer (they are implicit), but are included in the reaction layer "/r" and transition state connectivity layer "/z" by necessity.

Composite reactions are written as a sequence in each layer. For example, CHF_2 + OH = CHFO + HF is a radical combination followed by a 1,2-elimination of HF. Table A3 shows the InChI-ER identifier for this composite reaction:

/vCHF2;HO;CHFO;FH; /c2-1-3;;2-1-3;; /h1H;h1H;h1H;h1H;

/r1+1';1,1'-2,2'; /z1-1';1-2-2'-1'-1; /kC-O(-1);CO-FH;

InChI-ER identifiers for all of the reactions in this mechanism are provided in Table A4.

References

[1] AR6 Climate Change 2021: The Physical Science Basis, International Panel on Climate Change (IPCC), Geneva, Switzerland, 2021, https://www.ipcc.ch/report/ar6/wg1/ (accessed July 22, 2021).

[2] V. Masson-Delmotte, P. Zhai, IPCC, 2018: Global warming of 1.5°C. An IPCC Special Report on the impacts of global warming of 1.5°C above pre-industrial levels and related global greenhouse gas emission pathways, in the context of strengthening the global response to the threat of climate

change, sustainable development, and efforts to eradicate poverty. , International Panel on Climate Change, Geneva, Switzerland, 2018.

[3] P.A. Domanski, R. Brignoli, J.S. Brown, A.F. Kazakov, M.O. McLinden, Low-GWP refrigerants for medium and highpressure applications, Int J Refrig 84 (2017) 198-209.

[4] M.O. McLinden, J.S. Brown, R. Brignoli, A.F. Kazakov, P.A. Domanski, Limited options for low-global-warming-potential refrigerants, Nat Commun 8 (2017).

[5] O. Hodnebrog, M. Etminan, J.S. Fuglestvedt, G. Marston, G. Myhre, C.J. Nielsen, K.P. Shine, T.J. Wallington, Global warming potentials and radiative efficiencies of halocarbons and related compounds: A comprehensive review, Rev Geophys 51 (2013) 300-378.

[6] I.H. Bell, P.A. Domanski, M.O. McLinden, G.T. Linteris, The hunt for nonflammable refrigerant blends to replace R-134a, Int J Refrig 104 (2019) 484-495.

[7] D.R. Burgess, Jr., J.A. Manion, Rate Constants for Abstraction of H from the Fluoromethanes by H, O, F, and OH, Journal of Physical and Chemical Reference Data, J Phys Chem Ref Data 50 (2021) 023102.

[8] D.R. Burgess, Jr., R.R. Burrell, V.I. Babushok, J.A. Manion, M.J. Hegetschweiler, G.T. Linteris, Burning velocities of R-32/O_2/N2 mixtures: Experimental measurements and development of a validated detailed chemical kinetic model, Combustion and Flame 236 (2022) 111795.

[9] D.R. Burgess, Jr., J.A. Manion, R.R. Burrell, V.I. Babushok, M.J. Hegetschweiler, G.T. Linteris, Development and Validation of a Mechanism for Flame Propagation in R32/Air Mixtures, Eastern States Section of the Combustion Institute, Spring Technical Meeting, (2018) March 4-7, 2018, State College, Pennsylvania.

[10] R.R. Burrell, J.L. Pagliaro, G.T. Linteris, Effects of stretch and thermal radiation on difluoromethane/air burning velocity measurements in constant volume spherically expanding flames, Proceedings of the Combustion Institute 37 (2019) 4231-4238.

[11] D.R. Burgess, Jr., J.A. Manion, R.R. Burrell, V.I. Babushok, M.J. Hegetschweiler, G.T. Linteris, Validated Model for Burning Velocities of R-32/O_2/N_2 Mixtures over a Wide Range of Conditions, 11th U. S. National Combustion Meeting (2019) March 24-27, 2019, Pasadena, CA.

[12] R.J.G. Kee, J. F.; Smooke, M. D.; Miller, J. A., PREMIX: A Fortran Program for Modeling Steady Laminar One-Dimensional Premixed Flames (Version 2.5b), Sandia National Laboratories, Livermore, California, 1992.

[13] G.P. Smith, D.M. Golden, M. Frenklach, N.W. Moriarty, B. Eiteneer, M. Goldenberg, C.T. Bowman, R.K. Hanson, S. Song, W.C. Gardiner, Jr., V.V. Lissianski, Z. Qin, GRI-Mech 3.0, http://combustion.berkeley.edu/gri-mech/ (accessed July 22, 2021), 1999.

[14] H. Wang, E. Dames, B. Sirjean, D.A. Sheen, R. Tango, A. Violi, J.Y.W. Lai, F.N. Egolfopoulos, D.F. Davidson, R.K. Hanson, C.T. Bowman, C.K. Law, W. Tsang, N.P. Cernansky, D.L. Miller, R.P. Lindstedt, JetSurf 2.0, http://web.stanford.edu/group/haiwanglab/JetSurF/JetSurF2.0/

(accessed July 22, 2021), 2009.

[15] J. Li, Z.W. Zhao, A. Kazakov, M. Chaos, F.L. Dryer, J.J. Scire, A comprehensive kinetic mechanism for CO, CH_2O, and CH_3OH combustion, Int J Chem Kinet 39 (2007) 109-136.

[16] C.D. Needham, P.R. Westmoreland, Combustion and flammability chemistry for the refrigerant HFO-1234yf (2,3,3,3-tetrafluoropropene), Combustion and Flame 184 (2017) 176-185.

[17] R.J. Kee, G. Dixon-Lews, J. Warnatz, R.E. Coltrin, J.S. Millrt, A Fortran Computer Code Package for the Evaluation of Gas-Phase, Multicomponent Transport Properties., Sandia National Laboratory), SAND86-8246. , (1986).

[18] R.C. Reid, J.M. Prausnitz, T.K. Sherwood, The Properties of Gases and Liquids McGraw-Hill, (1977).

[19] C. Avendano, T. Lafitte, C.S. Adjiman, A. Galindo, E.A. Muller, G. Jackson, SAFT-gamma Force Field for the Simulation of Molecular Fluids: 2. Coarse-Grained Models of Greenhouse Gases, Refrigerants, and Long Alkanes, J Phys Chem B 117 (2013) 2717-2733.

[20] A.S. Teja, R.L. Smith, R.K. King, T.F. Sun, Correlation and prediction of the transport properties of refrigerants using two modified rough hard-sphere models, Int J Thermophys 20 (1999) 149-161.

[21] V.I. Babushok, D.R. Burgess, Jr., K.K. Kim, M.J. Hegetschweiler, G.T. Linteris, Modeling of Combustion of Fluorine-Containing Refrigerants, NIST Technical Note, (2021) in press.

[22] S. Takahashi, H. Nakamura, T. Tezuka, K. Maruta, Effects of blending ratios on the reactivities of CH_2F_2/C_2HF_5 refrigerant blends, Proceedings of the Combustion Institute 38 (2021) 2487-2495.

[23] G. Linteris, V. Babushok, Laminar burning velocity predictions for C-1 and C-2 hydrofluorocarbon refrigerants with air, J Fluorine Chem 230 (2020).

[24] V.I. Babushok, D.R. Burgess, M.J. Hegetschweiler, G.T. Linteris, Flame propagation in the mixtures of O_2/N_2 oxidizer with fluorinated propene refrigerants (CH_2CFCF_3, $CHFCHCF_3$, CH_2CHCF_3), Combust Sci Technol 193 (2020) 1949-1972.

[25] S. Takahashi, H. Nakamura, T. Tezuka, S. Hasegawa, K. Maruta, Multi-stage oxidation of a CH_2F_2/air mixture examined by weak flames in a micro flow reactor with a controlled temperature profile, Combustion and Flame 201 (2019) 140-147.

[26] W. Xu, Y. Jiang, R. Qiu, X.Y. Ren, Influence of halon replacements on laminar flame speeds and extinction limits of hydrocarbon flames, Combustion and Flame 182 (2017) 1-13.

[27] P. Papas, S. Zhang, W. Kim, S.P. Zeppieri, M.B. Colket, P. Verma, Laminar flame speeds of 2,3,3,3-tetrafluoropropene mixtures, Proceedings of the Combustion Institute 36 (2017) 1145-1154.

[28] C. Osorio, A. Morones, J.W. Hargis, E.L. Petersen, M.S. Mannan, Effect of C2HF5 and C3HF7 on methane and propane ignition and laminar flame speed: Experimental and numerical evaluation, J Loss Prevent Proc 48 (2017) 21-31.

[29] A. Matsugi, K. Takahashi, Thermal Decomposition of 2,3,3,3-and trans-1,33,3-Tetrafluoropropenes, J Phys Chem A 121 (2017) 4881-4890.

[30] V.I. Babushok, G.T. Linteris, Kinetic mechanism of 2,3,3,3-tetrafluoropropene (HFO-1234yf) combustion, J Fluorine Chem 201 (2017) 15-18.

[31] X.Y. Ren, Y. Jiang, W. Xu, Numerical investigation of the chemical and physical effects of halogenated fire suppressants addition on methane-air mixtures, J Fire Sci 34 (2016) 416-430.

[32] G.T. Linteris, D.R. Burgess, F. Takahashi, V.R. Katta, H.K. Chelliah, O. Meier, Stirred reactor calculations to understand unwanted combustion enhancement by potential halon replacements, Combustion and Flame 159 (2012) 1016-1025.

[33] X.M. Zhou, B. Zhou, Comprehensive Theoretical and Experimental Studies on the CF_3H Fire-extinguishing Mechanism, Chinese J Chem 29 (2011) 1335-1340.

[34] W.F. Han, E.M. Kennedy, S.K. Kundu, J.C. Mackie, A.A. Adesina, B.Z. Dlugogorski, Experimental and chemical kinetic study of the pyrolysis of trifluoroethane and the reaction of trifluoromethane with methane, J Fluorine Chem 131 (2010) 751-760.

[35] E. Ikeda, J.C. Mackie, An experimental and modelling study of ignition delays in shock-heated ethane-oxygen-argon mixtures inhibited by 2H-heptafluoropropane, Z Phys Chem 215 (2001) 997-1009.

[36] B.A. Williams, D.M. L'Esperance, J.W. Fleming, Intermediate species profiles in low-pressure methane/oxygen flames inhibited by 2-H heptafluoropropane: Comparison of experimental data with kinetic modeling, Combustion and Flame 120 (2000) 160-172.

[37] D. L'Esperance, B.A. Williams, J.W. Fleming, Intermediate species profiles in low pressure premixed flames inhibited by fluoromethanes, Combustion and Flame 117 (1999) 709-731.

[38] R.G. Hynes, J.C. Mackie, A.R. Masri, Shock-tube study of the pyrolysis of the halon replacement molecule CF_3CHFCF_3, J Phys Chem A 103 (1999) 54-61.

[39] Y. Saso, D.L. Zhu, H. Wang, C.K. Law, N. Saito, Laminar burning velocities of trifluoromethane-methane mixtures: Experiment and numerical simulation, Combustion and Flame 114 (1998) 457-468.

[40] G.T. Linteris, D.R. Burgess, V. Babushok, M. Zachariah, W. Tsang, P. Westmoreland, Inhibition of premixed methane-air flames by fluoroethanes and fluoropropanes, Combustion and Flame 113 (1998) 164-180.

[41] R.G. Hynes, J.C. Mackie, A.R. Masri, Inhibition of premixed hydrogen-air flames by 2-H heptafluoropropane, Combustion and Flame 113 (1998) 554-565.

[42] D.R. Burgess, V.I. Babushok, G.T. Linteris, J.A. Manion, A Chemical Kinetic Mechanism for 2-Bromo-3,3,3-trifluoropropene (2-BTP) Flame Inhibition, Int J Chem Kinet 47 (2015) 533-563.

[43] G.T. Linteris, L. Truett, Inhibition of premixed methane-air flames by fluoromethanes, Combustion and Flame 105 (1996) 15-27.

[44] D.R. Burgess, M.R. Zachariah, W. Tsang, P.R. Westmoreland, Thermochemical and chemical kinetic data for fluorinated hydrocarbons, Prog Energ Combust 21 (1995) 453-529.

[45] D.G. Goodwin, H.K. Moffat, R.L. Speth, Cantera: An object- oriented software toolkit for chemical kinetics, thermodynamics, and transport processes, 2017.

[46] D.R. Burgess, Jr., J. Racek, XSenkplot—An Interactive, Graphics Postprocesser for Numerical Simulations of Chemical Kinetics, National Institute of Standards and Technology, Gaithersburg, Maryland, 1996.

[47] B.N. Taylor, C. Kuyatt, Guidelines for Evaluating and Expressing the Uncertainty of NIST Measurement Results, NIST Technical Note 1297 (1994) 1.

[48] A. Ganyecz, M. Kallay, J. Csontos, High Accuracy Quantum Chemical and Thermochemical Network Data for the Heats of Formation of Fluorinated and Chlorinated Methanes and Ethanes, J Phys Chem A 122 (2018) 5993-6006.

[49] Active thermochemical tables (ATcT), version 1.122p. https://atct.anl.gov/Thermochemical%20Data/version%201.122p/ 2020).

[50] E. Paulechka, A. Kazakov, Enthalpy of formation of aqueous hydrofluoric acid: Revision needed?, J Chem Thermodyn 142 (2020).

[51] E. Paulechka, A. Kazakov, Critical Evaluation of the Enthalpies of Formation for Fluorinated Compounds Using Experimental Data and High-Level Ab Initio Calculations, J Chem Eng Data 64 (2019) 4863-4874.

[52] E. Goos, A. Burcat, B. Ruscic, Extended Third Millennium Thermodynamic Database for Combustion and Air-Pollution Use with updates from Active Thermochemical Tables. ftp://ftp.technion.ac.il/pub/supported/aetdd/thermodynamics/BURCAT.THR (accessed August 2012).

[53] M.R. Zachariah, P.R. Westmoreland, D.R.F. Burgess, W. Tsang, C.F. Melius, Theoretical prediction of thermochemical and kinetic properties of fluorocarbons, Acs Sym Ser 611 (1995) 358-373.

[54] M.R. Zachariah, W. Tsang, P.R. Westmoreland, D.R.F. Burgess, Theoretical Prediction of the Thermochemistry and Kinetics of Reactions of CF_2O with Hydrogen-Atom and Water, J Phys Chem 99 (1995) 12512-12519.

[55] A.G. Baboul, L.A. Curtiss, P.C. Redfern, K. Raghavachari, Gaussian-3 theory using density functional geometries and zero-point energies, J Chem Phys 110 (1999) 7650-7657.

[56] V. Mokrushin, V. Bedanov, W. Tsang, M.R. Zachariah, V.D. Knyazev, W.S. McGivern, ChemRate 1.5.10, 2011.

[57] R.A. Marcus, Unimolecular dissociations and free radical recombination reactions, J Chem Phys 20 (1952) 359-364.

[58] G.M. Wieder, R.A. Marcus, Dissociation and Isomerization of Vibrationally Excited Species .2. Unimolecular Reaction Rate Theory and Its Application, J Chem Phys 37 (1962) 1835.

[59] R.A. Marcus, Generalization of Activated Complex Theory of Reaction Rates .I. Quantum Mechanical Treatment, J Chem Phys 41 (1964) 2614.

[60] R.A. Marcus, W.L. Hase, K.N. Swamy, Rrkm and Non-Rrkm Behavior in Chemical Activation and Related Studies, J Phys Chem 88 (1984) 6717-6720.

[61] D.M. Wardlaw, R.A. Marcus, On the Statistical-Theory of Unimolecular Processes, Adv Chem Phys 70 (1988) 231-263.

[62] M. Goswami, R.J.M. Bastiaans, A.A. Konnov, L.P.H. de Goey, Laminar burning velocity of lean H2/CO mixtures at elevated pressure using the heat flux method, Int J Hydrogen Energ 39 (2014) 1485-1498.

[63] N.A. Slavinskaya, M. Abbasi, J.H. Starcke, R. Whitside, A. Mirzayeva, U. Riedel, W. Li, J. Oreluk, A. Hegde, A. Packard, M. Frenklach, G. Gerasimov, O. Shatalov, Development of an Uncertainty Quantification Predictive Chemical Reaction Model for Syngas Combustion, Energ Fuel 31 (2017) 2274-2297.

[64] C.D. Walther, H.G. Wagner, On the Reactions of F Atoms with H_2O, H_2O_2, and NH_3, Ber Bunsen Phys Chem 87 (1983) 403-409.

[65] P.S. Stevens, W.H. Brune, J.G. Anderson, Kinetic and Mechanistic Investigations of F+H_2O/D_2O and F+H_2/D_2 over the Temperature-Range 240-373-K, J Phys Chem 93 (1989) 4068-4079.

[66] R.J. Frost, D.S. Green, M.K. Osborn, I.W.M. Smith, Time-Resolved Vibrational Chemiluminescence - Rate Constants for the Reactions of F-Atoms with H_2O and HCN, and for the Relaxation of HF (v = 1) by H_2O and HCN, Int J Chem Kinet 18 (1986) 885-898.

[67] C. Anastasi, S. Beverton, T. Ellermann, P. Pagsberg, Reaction of CH_3 Radicals with OH at Room-Temperature and Pressure, J Chem Soc Faraday Trans 87 (1991) 2325-2329.

[68] T.L. Nguyen, J. Li, R. Dawes, J.F. Stanton, H. Guo, Accurate Determination of Barrier Height and Kinetics for the F + H_2O -> HF + OH Reaction, J Phys Chem A 117 (2013) 8864-8872.

[69] G. Leroy, M. Sana, A. Tinant, Theoretical-Study on the Hydrogen Abstraction Reactions RH+X Reverisble RH+X with R,X=H, CH_3, NH_2, OH and F, Can J Chem 63 (1985) 1447-1456.

[70] J. Li, Ring-Polymer Molecular Dynamics Studies of Thermal Rate Coefficients for Reaction F+H_2O -> HF+OH, Chinese J Chem Phys 32 (2019) 313-318.

[71] X.R. Zhang, J. Chen, X. Xu, S. Liu, D.H. Zhang, A neural network potential energy surface for the F + H_2O <-> HF plus OH reaction and quantum dynamics study of the isotopic effect, Phys Chem Chem Phys 23 (2021) 8809-8816.

[72] A. Persky, H. Kornweitz, The kinetics of the reaction F+H_2->HF+H. A critical review of literature data, Int J Chem Kinet 29 (1997) 67-71.

[73] E. Wurzberg, P.L. Houston, The Temperature-Dependence of Absolute Rate Constants for the F+H_2 and F+D_2 Reactions, J Chem Phys 72 (1980) 4811-4814.

[74] M.A.A. Clyne, A. Hodgson, Absolute Rate Constants for the Reaction of Fluorine-Atoms with H_2, CH_2Cl_2, CH_2ClF, CH_2F_2 and $CHCl_2$, J Chem Soc Farad T 2 81 (1985) 443-455.

[75] V.I. Igoshin, L.V. Kulakov, A.I. Nikitin, Determination of the rate constant of the chemical reaction F + H_2(D_2) = HF(DF) + H(D) from the stimulated emission of the HF(DF) molecules., Sov. J. Quant. Electron. 3 (1974) 306-311.

[76] D.M. Fasano, N.S. Nogar, The Infrared Chemi-luminescent Reaction of Cl Atoms With H_2CO, Int J Chem Kinet 13 (1981) 325-332.

[77] K.H. Homann, W.C. Solomon, J. Warnatz, H.G. Wagner, C. Zetzsch, Method for Producing Fluorine Atomes in Inert Gas, Ber. Bunsenges. Phys. Chem. 74 (1970) 585.

[78] R.F. Heidner, J.F. Bott, C.E. Gardner, J.E. Melzer, Absolute Rate Coefficients for F+H_2 and F+D_2 at T=295-765 K, J Chem Phys 72 (1980) 4815-4821.

[79] J.M. Preses, R.E. Weston, G.W. Flynn, IR Chemiluminescence from Hydrogen Halides Produced in IR Photodissociationd, Chem Phys Lett 48 (1977) 425-430.

[80] K.L. Kompa, J. Wanner, Study of Some Fluorine Atom Reactions using a Chemical Laser Method Chem Phys Lett 12 (1972) 560-+.

[81] I.B. Goldberg, G.R. Schneider, Kinetic Study of Reaction of F with H_2 and CF_3H by ESR Methods, J Chem Phys 65 (1976) 147-153.

[82] M.A. Ioffe, Y.M. Gershenzon, V.B. Rozenshtein, S.Y. Umanskii, Non-Arrhenius Behavior of ohe F+H_2 Reaction Rate At 293-700 K, Chem Phys Lett 154 (1989) 131-134.

[83] Y. Bedjanian, Rate constants for the reactions of F atoms with H_2 and D_2 over the temperature range 220-960 K, Int J Chem Kinet 53 (2021) 527-535.

[84] Z.G. Sun, D.H. Zhang, Development of the Potential Energy Surface and Current Stage of the Quantum Dynamics Studies of the F+H_2/HD Reaction, Int J Quantum Chem 115 (2015) 689-699.

[85] D. De Fazio, S. Cavalli, V. Aquilanti, Benchmark Quantum Mechanical Calculations of Vibrationally Resolved Cross Sections and Rate Constants on ab Initio Potential Energy Surfaces for the F plus HD Reaction: Comparisons with Experiments, J Phys Chem A 120 (2016) 5288-5299.

[86] J. Chen, Z.G. Sun, D.H. Zhang, An accurate potential energy surface for the F + H_2 -> HF + H reaction by the coupled-cluster method, J Chem Phys 142 (2015).

[87] M. Moix, F. Huarte-Larranaga, Direct quantum mechanical calculation of the F+H_2 -> HF+H thermal rate constant, Chem Phys 351 (2008) 65-71.

[88] H.B. Wang, W.H. Thompson, W.H. Miller, "Direct" calculation of thermal rate constants for the F+H_2 -> HF+F reaction, J Phys Chem A 102 (1998) 9372-9379.

[89] R. Steckler, D.G. Truhlar, B.C. Garrett, Variational Transition-State Theory Calculations of the Reaction-Rates of F with H_2, D_2, and HD and the Intermolecular and Intramolecular Kinetic Isotope Effects, J Chem Phys 82 (1985) 5499-5505.

[90] V. Aquilanti, S. Cavalli, D. De Fazio, A. Volpi, A. Aguilar, J.M. Lucas, Benchmark rate constants by the hyperquantization algorithm. The F+H_2 reaction for various potential energy surfaces: features of the entrance channel and of the transition state, and low temperature reactivity, Chem Phys 308 (2005) 237-253.

[91] S. Gomez-Carrasco, L. Gonzalez-Sanchez, A. Aguado, M. Paniagua, O. Roncero, M.L. Hernandez, J.M. Alvarino, Dynamics and kinetics of the F+OH reaction on the ground triplet potential energy surface, Chem Phys Lett 383 (2004) 25-30.

[92] S.F. Politanskii, U.V. Shevchuk, Thermal conversions of fluoromethanes. II. Pyrolysis of difluoromethane and trifluoromethane, Kinetics and Catalysis 9 (1968) 411-417.

[93] C.J. Cobos, K. Hintzer, L. Solter, E. Tellbach, A. Thaler, J. Troe, Shock Wave and Theoretical Modeling Study of the Dissociation of CH_2F_2. I. Primary Processes, J Phys Chem A 121 (2017) 7813-7819.

[94] A. Matsugi, H. Shiina, Kinetics of the thermal decomposition of CH_2F_2, Chem Phys Lett 707 (2018) 140-143.

[95] J. Troe, V.G. Ushakov, Revisiting falloff curves of thermal unimolecular reactions, J Chem Phys 135 (2011).

[96] K.P. Schug, H.G. Wagner, F. Zabel, Gas-Phase Alpha,Alpha Elimination of Hydrogen Halides from Halomethanes .1. Thermal-Decomposition of Chlorodifluoromethane, Trifluoromethane, and Trichloromethane Behind Shock-Waves, Ber Bunsen Phys Chem 83 (1979) 167-175.

[97] A.W. Jasper, J.A. Miller, S.J. Klippenstein, Collision Efficiency of Water in the Unimolecular Reaction CH_4 (+H_2O) reversible arrow CH_3 + H (+H_2O): One-Dimensional and Two-Dimensional Solutions of the Low-Pressure-Limit Master Equation, J Phys Chem A 117 (2013) 12243-12255.

[98] G.O. Pritchard, M.J. Perona, Some hydrogen atom abstraction reactions of CF_2H and CFH_2 radicals, and the C-H bond dissociation energy in CF_2H_2, Int J Chem Kinet 1 (1969) 509-525.

[99] A.A. Westenberg, N. Dehaas, Rates of H+CH_3X Reactions, J Chem Phys 62 (1975) 3321-3325.

[100] A. Matsugi, H. Shiina, Kinetics of Hydrogen Abstraction Reactions from Fluoromethanes and Fluoroethanes, Bull Chem Soc Jpn 87 (2014) 890-901.

[101] A. Miyoshi, K. Ohmori, K. Tsuchiya, H. Matsui, Reaction-Rates of Atomic Oxygen with Straight Chain Alkanes and Fluoromethanes at High-Temperatures, Chem Phys Lett 204 (1993) 241-247.

[102] J.B. Burkholder, J. Sander, J.R. Abbat, R.E. Huie, C.E. Kolb, M.J. Kurylo, V.L. Orkin, D.M. Wilmouth, P.H. Wine, Chemical Kinetics and Photochemical Data for Use in Atmospheric Studies. JPL Publication 15-10. http://jpldataeval.jpl.nasa.gov.

[103] A. Persky, The temperature dependence of the rate constants for the reactions $F+CH_3F$ and $F+CH_2F_2$, Chem Phys Lett 376 (2003) 181-187.

[104] L. Wang, J.Y. Liu, Z.S. Li, Ab initio direct dynamics studies on the hydrogen abstraction reactions of CF(2)H(2) and CF(3)H with F atom, Chem Phys 351 (2008) 154-158.

[105] N.K. Srinivasan, M.C. Su, J.W. Sutherland, J.V. Michael, Reflected shock tube studies of high-temperature rate constants for CH_3+O_2, H_2CO+O_2, and $OH+O_2$, J Phys Chem A 109 (2005) 7902-7914.

[106] K. Takahashi, Y. Sekiuji, Y. Yamamori, T. Inomata, K. Yokoyama, Kinetic studies on the reactions of CF_3 with $O(^3P)$ and H atoms at high temperatures, J Phys Chem A 102 (1998) 8339-8348.

[107] Q. Luo, Q.S. Li, Direct ab initio dynamics study of the unimolecular reaction of CH_2FO, J Phys Chem A 108 (2004) 5050-5056.

[108] J.A. Seetula, I.R. Slagle, D. Gutman, S.M. Senkan, Kinetics of the reaction of the CCl_3 radical with oxygen atoms, Chem Phys Lett 252 (1996) 299-303.

[109] S.I. Stoliarov, A. Bencsura, E. Shafir, V.D. Knyazev, I.R. Slagle, Kinetics of the reaction of the $CHCl_2$ radical with oxygen atoms, J Phys Chem A 105 (2001) 76-81.

[110] N.K. Srinivasan, M.C. Su, J.V. Michael, S.J. Klippenstein, L.B. Harding, Reflected shock tube and theoretical studies of high-temperature rate constants for $OH+CF_3H$ -> CF_3+H_2O and CF_3+OH -> Products, J Phys Chem A 111 (2007) 6822-6831.

[111] A.W. Jasper, S.J. Klippenstein, L.B. Harding, Theoretical rate coefficients for the reaction of methyl radical with hydroperoxyl radical and for methylhydroperoxide decomposition, Proceedings of the Combustion Institute 32 (2009) 279-286.

[112] R.J. Cvetanovic, Evaluated Chemical Kinetic Data for the Reactions of Atomic Oxygen $O(^3P)$ with Unsaturated-Hydrocarbons, J Phys Chem Ref Data 16 (1987) 261-326.

[113] D.S. Jones, S.J. Moss, Arrhenius Parameters for Reactions of Oxygen-Atoms with Fluorinated Ethylenes, Int J Chem Kinet 6 (1974) 443-452.

[114] H. Umemoto, K. Sugiyama, S. Tsunashima, S. Sato, The Arrhenius Parameters for the Reactions of O Atoms with Ethene and 5 Fluoroethenes, Bull Chem Soc Jpn 58 (1985) 1228-1233.

[115] J.R. Gilbert, I.R. Slagle, R.E. Graham, D. Gutman, Direct Identification of Reactive Routes and Measurement of Rate Constants in Reactions of Oxygen-Atoms with Fluoroethylenes, J Phys Chem 80 (1976) 14-18.

[116] S.Y. Lee, H.S. Yoo, W.K. Kang, K.H. Jung, Reaction of O(^{3}P) atoms with CF2=CXY (X,Y=H,F,Cl,Br). Discharge flow-chemiluminescence imaging technique, Chem Phys Lett 257 (1996) 415-420.

[117] E.L. Keating, R.A. Matula, High-Temperature Oxidation of Tetrafluoroethylene, J Chem Phys 66 (1977) 1237-1244.

[118] S.K. Zhou, M.S. Zhan, Y.W. Qiu, S.H. Liu, J.L. Shi, F.L. Li, J.X. Yao, Chemi-Luminescence of $CF_2(^3b_1)$ Produced by the Reaction O(^{3}P)+C_2F_4, Chem Phys Lett 121 (1985) 395-399.

[119] K.K. Murray, D.G. Leopold, T.M. Miller, W.C. Lineberger, Photoelectron-Spectroscopy of the Halocarbene Anions HCF-, HCCl-, HCBr-, HCl-, CF_2-, and CCl_2-, J Chem Phys 89 (1988) 5442-5453.

[120] C.P. Tsai, D.L. Mcfadden, Gas-Phase Atom Radical Kinetics of Atomic-Hydrogen, Nitrogen, and Oxygen Reactions with CHF Radicals, J Phys Chem 94 (1990) 3298-3300.

[121] N.K. Srinivasan, M.C. Su, J.V. Michael, A.W. Jasper, S.J. Klippenstein, L.B. Harding, Thermal decomposition of CF_3 and the reaction of CF_2+OH -> CF_2O+H, J Phys Chem A 112 (2008) 31-37.

[122] J.C. Biordi, C.P. Lazzara, J.F. Papp, Flame Structure Studies of Bromotrifluoromethane-Inhibited Methane Flames .4. Reactions of Inhibitor-Related Species in Flames Containing Initially 1.1-Percent Bromo-Trifluoro-Methane, J Phys Chem 82 (1978) 125-132.

[123] C.J. Cobos, G. Knight, L. Solter, E. Tellbach, J. Troe, Shock Wave and Theoretical Modeling Study of the Dissociation of CH_2F_2. II. Secondary Reactions, J Phys Chem A 121 (2017) 7820-7826.

[124] J.C. Biordi, C.P. Lazzara, J.F. Papp, Mass-Spectrometric Observation of Difluorocarbene and Its Reactions in Inhibited Methane Flames, J Phys Chem 80 (1976) 1042-1048.

[125] Y. Yamamori, K. Takahashi, T. Inomata, Shock-tube studies on the reactions of $CF_2(X^1A_1)$ with O(^{3}P) and H atoms, J Phys Chem A 103 (1999) 8803-8811.

[126] K.R. Ryan, I.C. Plumb, Gas-phase reactions of CF_3 and CF_2 with hydrogen atoms: Their significance in plasma processing, Plasma Chemistry and Plasma Processing 4 (1984) 141.

[127] C.P. Tsai, D.L. Mcfadden, Gas-Phase Atom-Radical Kinetics of Atomic-Hydrogen Reactions with CF_3, CF_2, and CF Radicals, J Phys Chem 93 (1989) 2471-2474.

[128] K.R. Ryan, I.C. Plumb, Gas-Phase Reactions of CF_2 with O(^{3}P) to produce COF: Their significance in plasma processing, Plasma Chem. Plasma Process. 4 (1984) 271-283.

[129] G. Hancock, P.D. Harrison, A.J. Macrobert, Rate-Constant Measurement of the O(^{3}P)+$CF_2(X^1A_1)$ Reaction, J Chem Soc Farad T 2 82 (1986) 647-651.

[130] C. Tsai, D.L. Mcfadden, Gas-Phase Atom Radical Kinetics of N-Atom and O-Atom Reactions with CF and CF_2 Radicals, Chem Phys Lett 173 (1990) 241-245.

[131] K. Yamasaki, A. Tanaka, A. Watanabe, K. Yokoyama, I. Tokue, Rate Constants for the Reactions $CF_2((X^1A_1, v_2=0$ and 1)+O Determined by a Photodissociation Laser-Induced Fluorescence Technique, J Phys Chem 99 (1995) 15086-15092.

[132] B. Vetters, B. Dils, T.L. Nguyen, L. Vereecken, S.A. Carl, J. Peeters, Absolute rate coefficients over extended temperature ranges and mechanisms of the $CF(X^2Pi)$ reactions with F_2, Cl_2 and O_2, Phys Chem Chem Phys 11 (2009) 4319-4325.

[133] J. Peeters, J. Vanhoeymissen, S. Vanhaelemeersch, D. Vermeylen, Absolute Rate-Constant Measurements of $CF(X^2Pi)$ Reactions .1. Reactions with O_2, F_2, Cl_2, and NO, J Phys Chem 96 (1992) 1257-1263.

[134] J. Vanhoeymissen, I. Deboelpaep, W. Uten, J. Peeters, Absolute Rate-Constant Measurements of $CF(X^2Pi)$ Reactions .2. Reactions with O, N, NO_2, N_2, N_2O, F, and C_3H_4, J Phys Chem 98 (1994) 3725-3731.

[135] T.P. Booth, G. Hancock, N.D. Perry, M. Toogood, 10th International Symposium on Gas Kinetics, Swansea, I.K., 1988.

[136] J.C. Biordi, C.P. Lazzara, J.F. Papp, Flame Structure Studies of CF_3Br-Inhibited Methane Flames .3. Effect of 1% CF_3Br on Composition, Rate Constants, and Net Reaction-Rates, J Phys Chem 81 (1977) 1139-1145.

[137] H. Richter, J. Vandooren, P.J. Vantiggelen, Kinetics of the Consumption of CF_3H, CF_2HCl and CF_2O in H_2/O_2 Flames, J Chim Phys Physicochim Biol 91 (1994) 1748-1762.

[138] K. Saito, H. Kuroda, T. Kakumoto, H. Munechika, I. Murakami, Thermal Unimolecular Decomposition of Formyl Fluoride in Ar, Chem Phys Lett 113 (1985) 399-402.

[139] A. Gahlaut, M. Paranjothy, Theoretical investigation of the dissociation chemistry of formyl halides in the gas phase, Phys Chem Chem Phys 22 (2020) 20069-20077.

[140] J.J. Zhong, W.W. Wang, Q. Li, W.W. Xia, Y. Shao, L. Yao, S.H. Lin, Anharmonic Effect of the Unimolecular Dissociation of HFCO and DFCO, J Chin Chem Soc-Taip 62 (2015) 582-591.

[141] S. Anand, H.B. Schlegel, Unimolecular dissociation of formyl halides HXCO -> CO+HX (X = F, Cl): An ab initio direct classical trajectory study, J Phys Chem A 106 (2002) 11623-11629.

[142] W.H. Fang, R.Z. Liu, Ab initio studies of dissociation pathways on the ground- and excited-state potential energy surfaces for HFCO, J Chem Phys 115 (2001) 5411-5417.

[143] T. Yamamoto, S. Kato, Theoretical study of the dissociation reaction HFCO->HF+CO: New ab initio potential function and classical trajectory analysis, J Chem Phys 107 (1997) 6114-6122.

[144] T.G. Wei, R.E. Wyatt, Analytical Potential Surface for the HFCO =>HF+CO Unimolecular Reaction, J Phys Chem 97 (1993) 13580-13585.

[145] J.S. Francisco, Y. Zhao, Abinitio Studies of Dissociation Pathways on the Ground-State Potential-Energy Surface for HFCO and HClCO, J Chem Phys 96 (1992) 7587-7596.

[146] Y.S. Choi, C.B. Moore, State-Specific Unimolecular Reaction Dynamics of HFCO .1. Dissociation Rates, J Chem Phys 97 (1992) 1010-1021.

[147] W. Tsang, R.F. Hampson, Chemical Kinetic Data Base for Combustion Chemistry. Part I. Methane and Related-Compounds, J Phys Chem Ref Data 15 (1986) 1087-1279.

[148] R.B. Klemm, E.G. Skolnik, J.V. Michael, Absolute Rate Parameters for the Reaction of $O(^3P)$ with H_2CO over the Temperature-Range 250 to 750 K, J Chem Phys 72 (1980) 1256-1264.

[149] T.J. Wallington, M.D. Hurley, Atmospheric Chemistry of HC(O)F - Reaction with OH Radicals, Environ Sci Technol 27 (1993) 1448-1452.

[150] J.S. Francisco, An Examination of Substituent Effects on the Reaction of OH Radicals with HXCO (Where X = H, F, and Cl), J Chem Phys 96 (1992) 7597-7602.

[151] C.Y. Wang, Q.S. Li, Theoretical study and rate constant computation on the reaction HFCO+OH -> CFO+H_2O, J Phys Chem A 112 (2008) 419-424.

[152] E.H. Appelman, M.A.A. Clyne, Reaction-Kinetics of Ground-State Fluorine, $F(^2P)$, Atoms .2. Reactions Forming Inorganic Fluorides, Studied Mass Spectrometrically, J Chem Soc Farad Trans 1 71 (1975) 2072-2084.

[153] V.D. Knyazev, A. Bencsura, I.R. Slagle, Unimolecular decomposition of the FCO radical, J Phys Chem A 101 (1997) 849-852.

[154] The IUPAC International Chemical Identifier (InChI). http://www.iupac.org/inchi/ (accessed July 22, 2021).

[155] S. Heller, A. McNaught, S. Stein, D. Tchekhovskoi, I. Pletnev, InChI - the worldwide chemical structure identifier standard, J. Cheminfo. 5 (2013).

[156] J.M. Goodman, I. Pletnev, P. Thiessen, E. Bolton, S.R. Heller, InChI version 1.06: now more than 99.99% reliable, J. Cheminfo. 13 (2021).

[157] D.R. Burgess, J.A. Manion, C.J. Hayes, Data Formats for Elementary Gas Phase Kinetics, Part 3: Reaction Classification, Int J Chem Kinet 47 (2015) 361-378.

[158] D.R. Burgess, J.A. Manion, C.J. Hayes, Data Formats for Elementary Gas-Phase Kinetics: Part 2. Unique Representations of Reactions, Int J Chem Kinet 47 (2015) 334-350.

[159] D.R. Burgess, J.A. Manion, C.J. Hayes, Data Formats for Elementary Gas Phase Kinetics, Part 1: Unique Representations of Species at the Molecular Level, Int J Chem Kinet 46 (2014) 640-650.

Table 1. Thermodynamic properties of fluorine-containing hydrocarbon species considered in the kinetics model. $\Delta_f H0$ – standard enthalpy of formation, U – expanded standard uncertainty (2σ), $S°$ – entropy of formation at standard state, $C_p°$ – heat capacity at standard state.

Species	$\Delta_f H_0$(298 K) kJ/mol	U kJ/mol	S_0(298 K) J/mol/K	$C_p°$ (298 K) J/mol/K	Reference
CH_2F_2	−451.66	0.68	246.347	42.869	[48]
CH_2F	−30.39	0.50	229.665	42.869	[48]
CHF_2	−243.45	0.51	258.000	43.062	[48]
CHF	148.66	0.43	223.342	34.588	[49, 52]
CF_2	−194.06	0.41	240.831	38.915	[48]
CF	246.74	0.13	213.034	30.056	[49, 52]
CHFCHF[Z]	-309.66	0.9	268.723	58.349	[49]
$CHFCF_2$	-498.2	1.6	292.665	69.191	[49]
C_2HF	105.66	0.41	231.573	52.268	[49]
CHFO	-382.23	0.31	246.727	40.019	[49, 52]
CF_2O	-606.45	0.41	258.971	47.365	[49, 52]
CFO	-176.04	0.37	248.992	38.880	[49, 52]

Table 2. Rate Expressions for Reactions for Combustion of CH_2F_2

Parameterized as $k = A\ T^n \exp(-E_a/RT)$. Units in mol, cm^3, s, kJ, K and f is uncertainty factor (95 % confidence limit). In some cases, both a two parameter (n=0) Arrhenius expression (valid only at combustion temperatures, i.e. typically 1200 K to 1800 K) and the three parameter extended Arrhenius expression (valid at both combustion and low temperatures) are given. The two parameter Arrhenius expressions are useful for comparing A factors and activation energies E_a. Where we could not determine a rigorous uncertainty estimate, we employed f = 2.0. Uncertainties denoted "ul" are where we have assigned upper limits to rate constants to which our model is not sensitive. The final column briefly indicates key references, applicable temperature ranges, and sometimes other metadata (see footnote). Unless otherwise noted, the temperature ranges of validity are assumed to be (300 to 1800) K. The most reliable range for each reaction, however, is the region in which it was experimentally determined. For details the reader should refer to the text.

Reaction	A	n	E	f	Reference †
H/O/F					
$H_2O + F \rightarrow OH + HF$	1.3×10^{8}	1.6	-4.6	1.4	this work, evaluation 200-1800 K [65] [68]
$H_2 + F \rightarrow H + HF$	6.6×10^{11}	0.7	2.2	1.4	this work, evaluation 200-1800 K [72]
$OH + F \rightarrow O + HF$	1.4×10^{12}	0.5	0	1.3	this work, evaluation [64]
$HO_2 + F \rightarrow O_2 + HF$	2.9×10^{12}	0.5	0	1.4	this work, evaluation [64]
CH_2F_2					
CH_2F_2 (+M) $\rightarrow$ CHF + HF (+M) F_c=0.08 H_2O/6.0/ CH_2F_2/2.0/ H_2/2.0/ CO_2/2.0/ HF/2.0/ CO/1.5/	2.25×10^{15} 9.80×10^{17}	0 0	342.3 261.9	1.6	k_∞, this work, adj in model [8] ‡ k_0, this work, adj in model [8] ‡
$CH_2F_2 + H \rightarrow CHF_2 + H_2$	8.29×10^{4}	2.63	30.65	1.5	this work, evaluation [7]
	2.49×10^{15}	0	62.54	1.5	this work, fit 1200-1800 K [7]
$CH_2F_2 + O \rightarrow CHF_2 + OH$	4.10×10^{5}	2.40	27.19	1.4	this work, evaluation [7]
	1.86×10^{14}	0	56.32	1.4	this work, fit 1200-1800 K [7]
$CH_2F_2 + OH \rightarrow CHF_2 + H_2O$	3.29×10^{6}	1.86	7.52	1.5	this work, evaluation [7]
	1.68×10^{13}	0	30.09	1.5	this work, fit 1200-1800 K [7]
$CH_2F_2 + F \rightarrow CHF_2 + HF$	2.05×10^{8}	1.79	1.30	1.35	this work, evaluation [7]
	5.54×10^{14}	0	9.77	1.35	this work fit 1200-1800 K [7]

CHF_2					
$CHF_2 + O_2 \rightarrow CF_2O + OH$	$7.5x10^{10}$	0	15	1.8	this work, adj in model, 1200-1800 K [8]
	$1.5x10^{7}$	1.0	0	1.8	this work, fit, 800-1800 K
$CHF_2 + H \rightarrow CHF + HF$	$6.5x10^{13}$	0	0	ul	this work, CF_3+H, est upper limit [106]
$CHF_2 + O \rightarrow CF_2O + H$	$3.7x10^{13}$	0	0	2.5	this work, est CF_3+O [106] δ=2.4
$CHF_2 + OH \rightarrow CHFO + HF$	$5.0x10^{13}$	0	0	1.5	this work, est upper limit, CF_3+OH[110]
$CHF_2 + F \rightarrow CF_2 + HF$	$3.0x10^{13}$	0	0	ul	this work, est upper limit, CHF_2+H
$CHF_2 + HO_2 \rightarrow CH_2F_2 + O_2$	$1.3x10^{13}$	0	21	ul	this work, est upper limit, CHF_2+H
$CHF_2 + CHF_2 \rightarrow CHFCF_2 + HF$	$3.1x10^{19}$	-1.95	17	1.5	RRKM [44] δ=1.4, est upper limit
	~$5x10^{12}$	0	0	1.5	this work, average 1200-1800 K
CHF					
$CHF + O_2 \rightarrow CHFO + O$	$3.4x10^{13}$	0	33	1.8	this work, adjusted in model [8]
$CHF + H_2O \rightarrow CH_2O + HF$	$5.0x10^{12}$	0	27	2.0	BAC-MP4 [53]
$CHF + H \rightarrow CH + HF$	$2.0x10^{14}$	0	0	2.0	[120] est branching 2:1
$CHF + H \rightarrow CF + H_2$	$1.0x10^{14}$	0	0	2.0	[120] est branching 2:1
$CHF + O \rightarrow CO + HF$	$9.0x10^{13}$	0	0	2.0	[120]
$CHF + OH \rightarrow CHFO + H$	$2.0x10^{13}$	0	0	2.0	est, CF_2+OH [121] δ=2
$CHF + OH \rightarrow HCO + HF$	$4.0x10^{12}$	0	0	2.0	[122]
$CHF + F \rightarrow CF + HF$	$1.0x10^{13}$	0	0	ul	this work, est upper limit
$CHF + CHF \rightarrow C_2HF + HF$	$2.7x10^{13}$	0	-21	ul	this work, est upper limit [44]
$CH_2F_2 + CHF \rightarrow$ CHFCHF[Z] + HF	$1.5x10^{13}$	0	84	ul	this work, est upper limit
CF_2					
$CF_2 + O_2 \rightarrow CF_2O + O$	$6.6x10^{7}$	1.5	94	1.5	this work, 1700-2500 K [117] adjusted in model [117] [8] δ=1/1.24
	$1.7x10^{13}$	0	111	1.5	this work, fit 1200-1800 K
$CF_2 + H_2O \rightarrow CHFO + HF$	$5.0x10^{12}$	0	105	2.0	BAC-MP4 [44]
$CF_2 + H \rightarrow CF + HF$	$3.6x10^{13}$	0	18	1.8	this work, fit 1200-1800 K
	$1.12x10^{10}$	1.0	8.5	1.8	this work, fit [125] [126] 300-2000 K
$CF_2 + O \rightarrow CFO + F$	$2.45x10^{13}$	0	0	2.0	1200-1800 K [125]
	$1.1x10^{12}$	0.4	0	2.0	[125, 128-131] 300-2000 K
$CF_2 + OH \rightarrow CF_2O + H$	$9.6x10^{13}$	0	0	1.5	[121] 1200-1800 K
	$2.1x10^{11}$	0.5	0	1.5	this work, fit 800-2000 K
$CF_2 + OH \rightarrow CFO + HF$	$2.0x10^{13}$	0	0	1.5	est upper limit [122] 1200-1800 K
CF					
$CF + O_2 \rightarrow CFO + O$	$6.6x10^{12}$	0	7.1	1.7	[132]
$CF + O \rightarrow CO + F$	$8.0x10^{13}$	0	5.9	1.6	[130]
$CF + OH \rightarrow CO + HF$	$8.0x10^{13}$	0	5.9	1.6	[130]
CHFO, CF_2O, CFO					
$CHFO + M \rightarrow CO + HF + M$	$2.5x10^{25}$	-3.0	180	2.0	[44]

CHFO + H → CFO + H_2	1.10×10^{8}	1.77	12.6	2.0	[44]
CHFO + O → CFO + OH	9.0×10^{12}	0	12.9	2.0	[44]
CHFO + OH → CFO + H_2O	2.8×10^{13}	0	27.7	2.0	[150]
CHFO + F → CFO + HF	2.7×10^{13}	0	7.5	2.0	[150]
CF_2O + H → CFO + HF	5.50×10^{8}	1.42	79	2.0	[54], path 1 via CF_2OH, (~90 %)
CF_2O + H → CFO + HF	1.2×10^{10}	0.83	93	2.0	[54], path 2 via CHF_2O, (~9 %)
CF_2O + H → CFO + HF	2.4×10^{7}	1.88	150	2.0	[54], path 3 via direct abstraction, (~1 %)
CFO + M → CO + F + M	3.0×10^{18}	-1.0	126	2.0	this work, fit [153]
CFO + F → CF_2O	1.0×10^{12}	0	0	2.0	[44] est upper limit
CHFCHF[*Z*], $CHFCF_2$					
CHFCHF[*Z*] + O → CH_2F + CFO	7.0×10^{9}	1.0	6.7	2.0	this work, fit [112] [113] n=1
$CHFCF_2$ + O → CHFO + CF_2	4.2×10^{8}	1.3	1.0	2.0	this work, fit [114] n=1.3 δ=2.5
	2.1×10^{13}	0	16.8	2.0	this work, fit 1200-1800 K
$CHFCF_2$ + O → CFO + CHF_2	3.4×10^{8}	1.3	1.0	2.0	this work, CHFO+CF_2, δ=0.8
	1.6×10^{13}	0	16.7	2.0	this work, fit 1200-1800 K
$CHFCF_2$ + O → CF_2O + CHF	2.5×10^{8}	1.3	1.0	2.0	this work, CHFO+CF_2, δ=0.6
	1.2×10^{13}	0	16.7	2.0	this work, fit 1200-1800 K

Table 2 Footnotes

† Indicated are main references used, applicable temperature ranges, methodology, and other metadata: if given, *x*+*y* refers to a reaction used to derive a rate by analogy; δ is an *a priori* or model-based adjustment factor used to modify the initial pre-exponential factor, *A*; est = estimate.

‡ k_∞ and k_0 used in complex (*P*,*T*) rate expression $k = k_\infty (P_r/1+P_r) F(P_r)$, where $P_r = k_0[M]/k_\infty$ is a reduced pressure, [M] is the concentration of the mixture including third-body efficiencies, and $F(P_r)$ a broadening function using the Troe form with a broadening factor of F_c. [95] k_∞ and k_0 from this work, fit to literature data and subsequently optimized to our burning velocity data. An optimized collision efficiency of 2.0 was used for CH_2F_2. Third-body efficiencies for other major species are also given.

Table A1. Species Identifiers

Species	InChI	CASRN	PubChem CID
CH_2F_2	CH2F2/c2-1-3/h1H2	75-10-5	6345
CH_2F	CH2F/c1-2/h1H2	3744-29-4	59907226
CHF_2	CHF2/c2-1-3/h1H	2670-13-5	137670
CHF	CHF/c1-2/h1H	13453-52-6	n/a
CF_2	CF2/c2-1-3	2154-59-8	n/a
CF	CF/c1-2	3889-75-6	162214211
CHFCHF[Z]	C2H2F2/c3-1-2-4/h1-2H/b2-1-	1630-77-9	5462921
$CHFCF_2$	C2HF3/c3-1-2(4)5/h1H	359-11-5	9665
C_2HF	C2HF/c1-2-3/h1H	2713-09-9	32759
CHFO	CHFO/c2-1-3/h1H	1493-02-3	15153
CF_2O	CF2O/c2-1(3)4	353-50-4	9623
CFO	CFO/c2-1-3	1871-24-5	137241

This is the author manuscript accepted for publication and has undergone full peer review but has not been through the copyediting, typesetting, pagination and proofreading process, which may lead to differences between this version and the Version of Record. Please cite this article as doi: 10.1002/kin.21549.

Table A2. InChI-ER layers

Layer	Description
/v	molecular formula for each of the reactants and products
/c	molecular connectivity for all of the heavy atoms (non-hydrogen atoms) in each of the reactants and products
/h	identifies the number of hydrogens on each species in the chemical reaction
/r	identifies the connectivity (bonds broken and formed) during the reaction (spectator atoms not involved in the reaction are not included)
/b	identifies (double bond) stereochemical isomers zusammen (Z) or entgagen (E)
/z	provides the connectivity of the atoms in the transition state (again, spectator atoms are not included)
/k	specific class of chemical reaction. • for example, "/kC-H+O" denotes an hydrogen (H) abstraction from a carbon-center (C) by an oxygen-center on a species (O), such as, $CH_2F_2 + OH = CHF_2 + H_2O$ • for example, "/kO.C-H" denotes a beta scission of H from a C adjacent to a O-centered radical site, such as, H-CH2O* = CH2O + H. A beta scission creates an unsaturation bond (or a lone pair such as a carbene, (e.g., :CHF).

Table A3. An example of InChI-ER for $CHF_2 + OH = CHFO + HF$

/v /c /h	molecular formula, connectivity, and location/number of hydrogens
/r1+1';1,1'-2,2'	atom 1 on first reactant combining with atom 1' on the second reactant followed by elimination of FH (2,2') from the carbon and oxygen centers on the chemically-activated intermediate CHF2-OH species (1,1')
/z1-1';1-1'-2'-2-1	the first term denotes the connectivity of the C-O "transition state" and the second term denotes the -(C-O-H-F-C)- four-centered transition state (the last carbon shown here is the first carbon)
/kC-O(-1);CO-HF	combination of a carbon-center with an oxygen-center, denoted as "C-O(-1)" - combinations are considered as the reverses of bond fissions (the unimolecular direction)

Table A4. InChI-ER Reaction Identifiers for this Mechanism

Reactants	→ Products	InChI-ER
H/O/F		
H_2O + F	→ OH + HF	/vH2O;F;HO;FH; /c;;;; /h1H2;;h1H;h1H; /r1-2-1'; /z1-2-1'; /kO-H+F; (abstraction)
H_2 + F	→ H + HF	/vH2;F;H;FH; /c; /h1H;;;h1H; /r1'-2'+1; /z1'-2'-1; /kH-H+F; (abstraction)
OH + F	→ O + HF	/vHO;F;O;FH; /c;;;; /h1H;;;h1H; /r1'-2'+1; /z1'-2'-1; /kO.H-F; (disproportionation)
HO_2 + F	→ O_2 + HF	/vHO2;F;O2;FH; /c1-2;;1-2;; /h1H;;;h1H; /r1'-3'+1; /k1'-3'-1; /kO.H+F; (disproportionation)
CH_2F_2		
CH_2F_2	→ CHF + HF	/vCH2F2;CHF.FH; /c2-1-3;c1-2;; /h1H2;h1H;1H; /r1-2,4 /z1-2-4-1 /kC-FH (1,1-elimination)
CH_2F_2 + H	→ CHF2 + H2	/vCH2F2.H;CHF2.H2; /c2-1-3;2-1-3; /h1H2;h1H;1H /r1-4+1' /z1-4+1' /kC-H+H /wCHF2 (abstraction)
CH_2F_2 + O	→ CHF_2 + OH	/vCH2F2;O;CHF2;HO; /c2-1-3;;2-1-3;; /h1H2;;h1H;h1H; /r1-4+1'; /z1-4-1'; /kC-H+O; (abstraction)
CH_2F_2 + OH	→ CHF_2 + H_2O	/vCH2F2;HO;CHF2;H2O;/c2-1-3;;2-1-3;; /h1H2;h1H;h1H;h1H2; /r1-4+1'; /z1-4-1'; /kC-H+O; (abstraction)
CH_2F_2 + F	→ CHF_2 + HF	/vCH2F2;F;CHF2;FH; /c2-1-3;;2-1-3;1-2;; /h1H2;;h1H;h1H; /r1-4+1'; /z1-4-1'; /kC-H+F; (abstraction)
CHF_2		
CHF_2 + O2	→ CF_2O + OH	/vCHF2;O2;CF2O;HO; /c2-1-3;1-2;2-1(3)4;; /h1H;h1H;h;h1H /r1+1';1-4+2';1-1'; /z1-1;1-4-2';1-1'; /kC-O(-1);C-H+O;C.O-O; (combination;isomerization;beta scission)
CHF_2 + H	→ CHF + HF	/vCHF2;H;CHF;FH; /c2-1-3;;1-2;; /h1H;;h1H;1H; /r1+1';1-2,1'; /z1-4-1';1-2-1'-1; /kC-H(-1);C-HF; (combination;1,1-elimination)
CHF_2 + O	→ CF_2O + H	/vCHF2;O;CF2O;H; /c2-1-3;;2-1(3)4;; /h1H;;;; /r1+1';1-4; /k1-1';1-4; /kC-O(-1);O.C-H; (combination;beta scission)
CHF_2 + OH	→ CHFO + HF	/vCHF2;HO;CHFO;FH; /c2-1-3;;2-1-3;; /h1H;h1H;h1H;h1H; /r1+1';1,1'-2,2'; /z1-1';1-2-2'-1'-1; /kC-O(-1);CO-FH; (combination;1,2-elimination)
CHF_2 + F	→ CF_2 + HF	/vCHF2;F;CF2;FH; /c2-1-3;;2-1-3;; /h1H;;;h1H; /r1+1';1-4,1'; /z1-4-1'-1; /kC-F(-1);C-HF; (combination;1,1-elimination)
CHF_2 + HO_2	→ CH_2F_2 + O_2	/vCHF2;O2;CH2F2;O2/c2-1-3;1-2;2-1-3;1-2; /h1H;h1H;h1H2;; /r1'-3'+1; /z1'-3'-1 /kO.O-H+C; (disproportionation)
CHF_2 + CHF_2	→ $CHFCF_2$ + HF	vCHF2;CHF2;C2HF3;FH; /c2-1-3;2-1-3;3-1-2(4)5;; /h1H;h1H;h1H;h1H; /r1+1';1,1'-4,2'; /z1-1';z1-1'-2'-4-1; /kC-C(-1);CC-HF; (combination;1,2-elimination)
CHF		
CHF + O_2	→ CHFO + O	/vCHF.O2;CHFO.O; /c1-2;1-2;2-1-3;;/h1H;;h1H;;

		/r1+1';1'-2'; /z1-1;1'-2'; /kC-O(-1);O.O-C; (combination;beta scission)
CHF + H_2O	→ CH_2O + HF	/vCHF;H2O;CH2O.FH; /c1-2;;1-2;1-2;; /h1H;1H2;h1H2;1H; /r1+1',2';1,1'-2,2'; /z1-1'-2'-1; /kC-OH(-1);CO-HF; (insertion;1,2-elimination)
CHF + H	→ CH + HF	/vCHF;H;CH;F; /c1-2;;1-2;; /h1H;;h1H;h1H; /r1+1';1-2,1'; /z1-1';1-2-1'-1; /kC-H(-1);C-HF; (combination;1,1-elimination)
CHF + H	→ CF + H_2	/vCHF;H;CF;H2; /c1-2;;1-2;; /h1H;;;h1H; /r1+1';r1-3,1'; /z1-3-1'-1; /kC-H(-1);C-HH; (combination;1,1-elimination)
CHF + O	→ CO + HF	/vCHF;O;CO.FH; /c1-2;;1-2;; /h1H;;;h1H; /r1+1';1-3,2'; /z1-1';1-3-2'-1; /kC-O(-1);C-HF; (combination;1,1-elimination)
CHF + OH	→ CHFO + H	/vCHF;HO;CHFO;H; /c1-2;;2-1-3;; /h1H;h1H;h1H;; /r1+1';1'-2'; /z1-1';1'-2'; /kC-O(-1);C.O-H; (combination;beta scission)
CHF + OH	→ HCO + HF	/vCHF;HO;CHO;FH; /c1-2;;1-2;; /h1H;h1H;h1H;h1H; /r1+1';1,1'-2,2'; /z1-1';1-1'-2'-2-1; /kC-O(-1);CO-HF; (combination;1,2-elimination)
CHF + F	→ CF + HF	/vCHF;F;CF;FH; /c1-2;;1-2;; /h1H;;;h1H; /r1-1';1-2',1'; /z1-2'-1'-1; /kC-F(-1);C-HF; (combination;1,1-elimination)
CHF + CHF	→ C_2HF + HF	/vCHF;CHF;C1-2-3;; /h1H;h1H;h1H;h1H; /r1-1';1,1'-2,2'; /z1-1'-2'-2-1; /kC-C(-1);CC-HF; (combination;;1,2-elimination)
CH_2F_2 + CHF	→ CHFCHF[*Z*] + HF	/vCH2F2;CHF;C2H2F2;FH; /c2-1-3;1-2;3-1-2-4;; /h1H2;h1H;h1-2H;h1H; /b2-1+; /r2'-1,4 /z2'-1-4-2'; /kC-CH(-1);CC-HF; (insertion;1,2-elimination)
CF_2		
CF_2 + O2	→ CF_2O + O	/vCF2;O2;CF2O;O; /c2-1-3;1-2;2-1(3)4;; /h;;;; /r1+1';1'-2'; /kC-O(-1);C.O-O; (combination;beta scission)
CF_2 + H_2O	→ CHFO + HF	/vCF2;H2O;CHFO;F; /c2-1-3;;c2-1-3;; /h;h1H2;h1H;h1H; /r1-1',2';1-1'-2'/z1-1'-2'-2-1; /kC-OH(-1);CO-HF; (insertion;1,2-elimination)
CF_2 + H	→ CF + HF	/vCF2;H;CF;FH; /c2-1-3;;1-2;; /h;;;h1H; /r1-2+1'; /z1-2=1'; /kC-F+H; (abstraction)
CF_2 + O	→ CFO + F	/vCF2;O;CFO;F; /c2-1-3;;2-1-3;; /h;;;; /kC-O;C-F (combination;bond fission)
CF_2 + OH	→ CF_2O + H	/vCF2;HO;CF2O;H; /c2-1-3;;2-1(3)4;; /h;h1H;;; /kC-O(-1);C.O-H; (combination;beta scission)
CF_2 + OH	→ CFO + HF	/vCF2.HO;CFO;FH; /c2-1-3;;2-1-3;; /h;h1H;;h1H; /kC-O(-1);C,O-F,H (combination;1,2-elimination)
CF		
CF + O_2	→ CFO + O	/vCF;O2;CFO;O; /c1-2;1-2;2-1-3;;/h;;;; /kC-O(-1);C.O-O) (combination;beta scission)
CF + O	→ CO + F	/vCF.O;CO.F;/c1-2;c1-2;/h;;;;

		/kC-O(-1);O.C-F (combination;beta scission)
CF + OH	→ CO + HF	/vCF.O; CO.F/c1-2;c1-2; h;;;h1H; /kC-O(-1);O.C-F (combination;beta scission)
CHFO, CF_2O, CFO		
CHFO	→ CO + HF	/vCHFO;CO.FH/c2-1-3;c1-2;/h1H;/h;1H /kC-H,F (1,1-elimination)
CHFO + H	→ CFO + H_2	/vCHFO.H;CFO.H2/c2-1-3;c2-1-3;/h1H;h;1H /kC-H+H (abstraction)
CHFO + O	→ CFO + OH	/vCHFO.O;CFO.HO/c2-1-3;c2-1-3;/h1H;h;1H; /kC-H+O (abstraction)
CHFO + OH	→ CFO + H_2O	/vCHFO.HO;CFO.O/c2-1-3;c2-1-3;/h1H;1H /kC-H+O (abstraction)
CHFO + F	→ CFO + HF	//vCHFO.F;CFO.FH;/c2-1-3;/h;1H; /kC-H+F (abstraction)
CF_2O + H	→ CFO + HF	/vCF2O.H;CFO.FH;/c2-1(3)4;c2-1-3;/h;1H /kC-H(-1);O.C-H,F (combination;1,1-elimination)
CF_2O + H	→ CFO + HF	/vCF2O.H;CFO.FH;/c2-1(3)4;c2-1-3;/h;1H; /kO-H;C,O-F,H (combination;1,2-elimination)
CF_2O + H	→ CFO + HF	/vCF2O.H;CFO.FH;/c2-1(3)4;2-1-3;/h;1H /kC-H+F (abstraction)
CFO	→ CO + F	/vCFO;CO.F;/c2-1-3;1-2;/h; /r1-2;/z1-2;/kO.C-F (beta scission)
CFO + F	→ CF_2O	/vCFO.F;CF2O;/c2-1-3;c2-1(3)4;/h; /r1+1'/z1-1'/kC+F (combination)
CHFCHF[Z], $CHFCF_2$		
CHFCHF[Z] + O	→ CH_2F + CFO	/vC2H2F2.O;CFO.CH2F;/c3-1-2-4;2-1-3;1-2; /h1-2H;/b2-1+;h;1H2; /kC.C-H;C.C-H;C.C-C; (addition;isomerization;beta scission)
$CHFCF_2$ + O	→ CHFO + CF_2	/vC2HF3.O;CF2.CHFO;/c3-1-2(4)5;c2-1-3;2-1-3;/h1H;h;1H; /r1+1';1-2; /z1-1';1-2; /kC+O;C.C-O (addition;beta scission)
$CHFCF_2$ + O	→ CFO + CHF_2	/vC2HF3.O;CHF2.CFO;/c3-1-2(4)5;2-1-3;2-1-3;/h1H;h1H; /kC+O;C.C-F;O.C-C (addition;isomerization;beta scission)
$CHFCF_2$ + O	→ CF_2O + CHF	/vC2HF3.O;CF2O.CHF/c3-1-2(4)5;2-1(3)4;1-2;/h1H;h;1H; /r2+1';1-2; /z2-1';1-2;/kC+O;C.C-O (addition;beta scission)

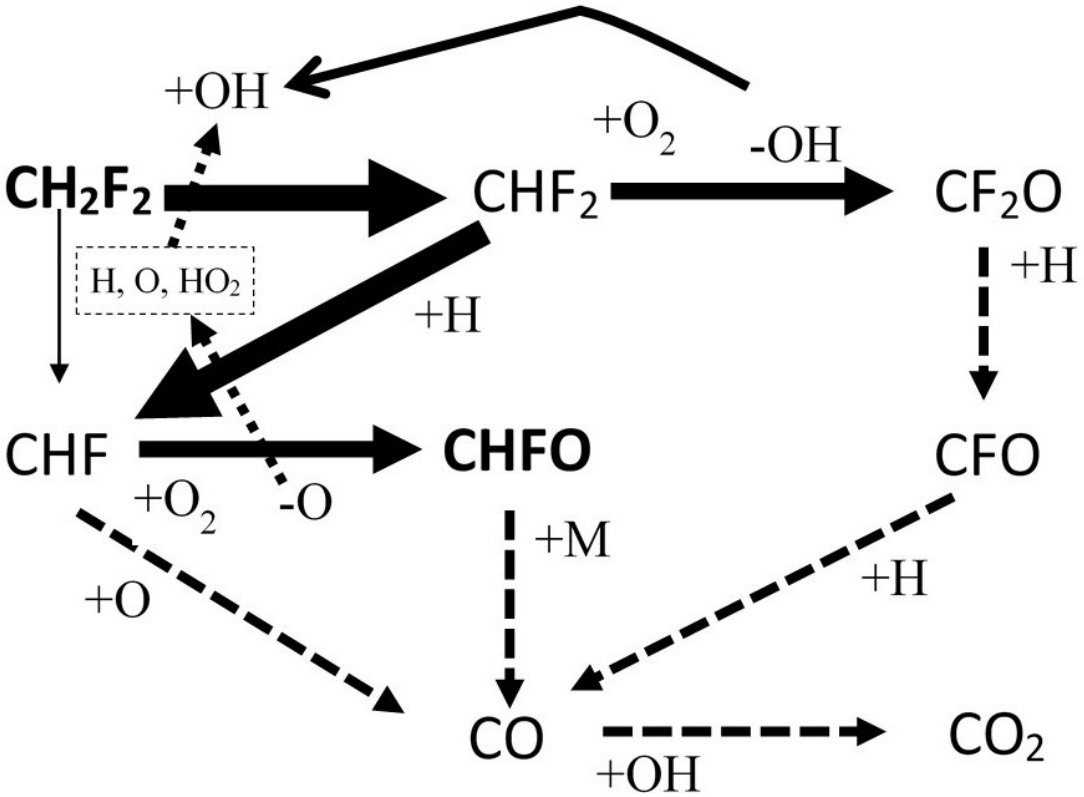

FIGURE 1 Low temperature (about 400 K to 900 K) pre-flame radical initiation phase. The thickness of the lines is a general indicator of the relative integrated fluxes. Carbon-containing species are shown along with H/O reactant partners. For clarity, HF and H/O species products are generally not shown in the figure. For example, "CHFO + M → CO" is shown, while the HF product is not; CO + OH → CO2 is shown, while the H product is not

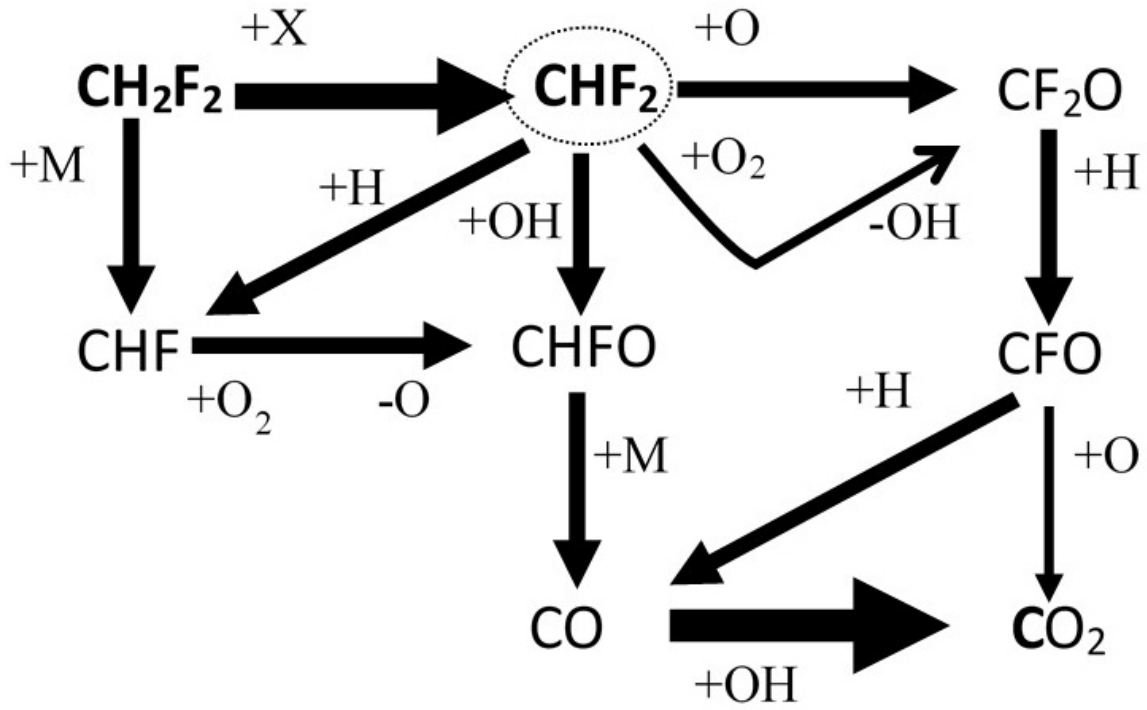

FIGURE 2 High temperature (about 1400 K to 2000 K) flame overall combustion pathway. The thickness of the lines is a general indicator of the relative integrated fluxes. Carbon-containing species are shown along with H/O reactant partners, but generally the HF and H/O species products are not shown for clarity in the figure

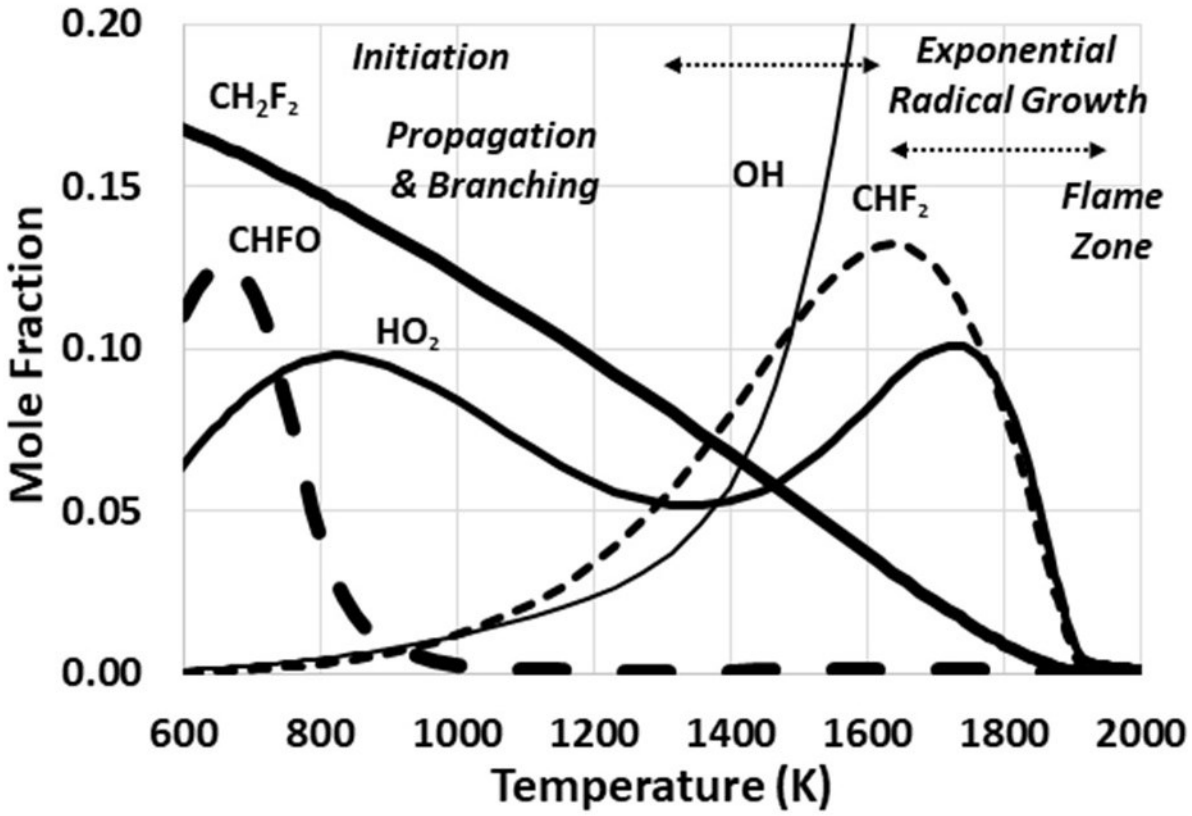

FIGURE 3 Concentration profiles for important species illustrating the two zones of chemistry. R-32/air, P = 1 bar, Tu = 298 K, □ = 1.1. Note that CHFO, HO2, OH, and CHF2 have been scaled by 120000, 5000, 5000, and 100, respectively, for ease in comparison. CHF is not shown here, but is an important intermediate between CH2F2 and CHFO in the initiation zone: CHF is formed slowly from CH2F2 and then rapidly forms CHFO via reaction with ambient O2 and subsequent loss of O. Figure 2 and figure 3 show the reaction pathways at low and high temperatures, respectively

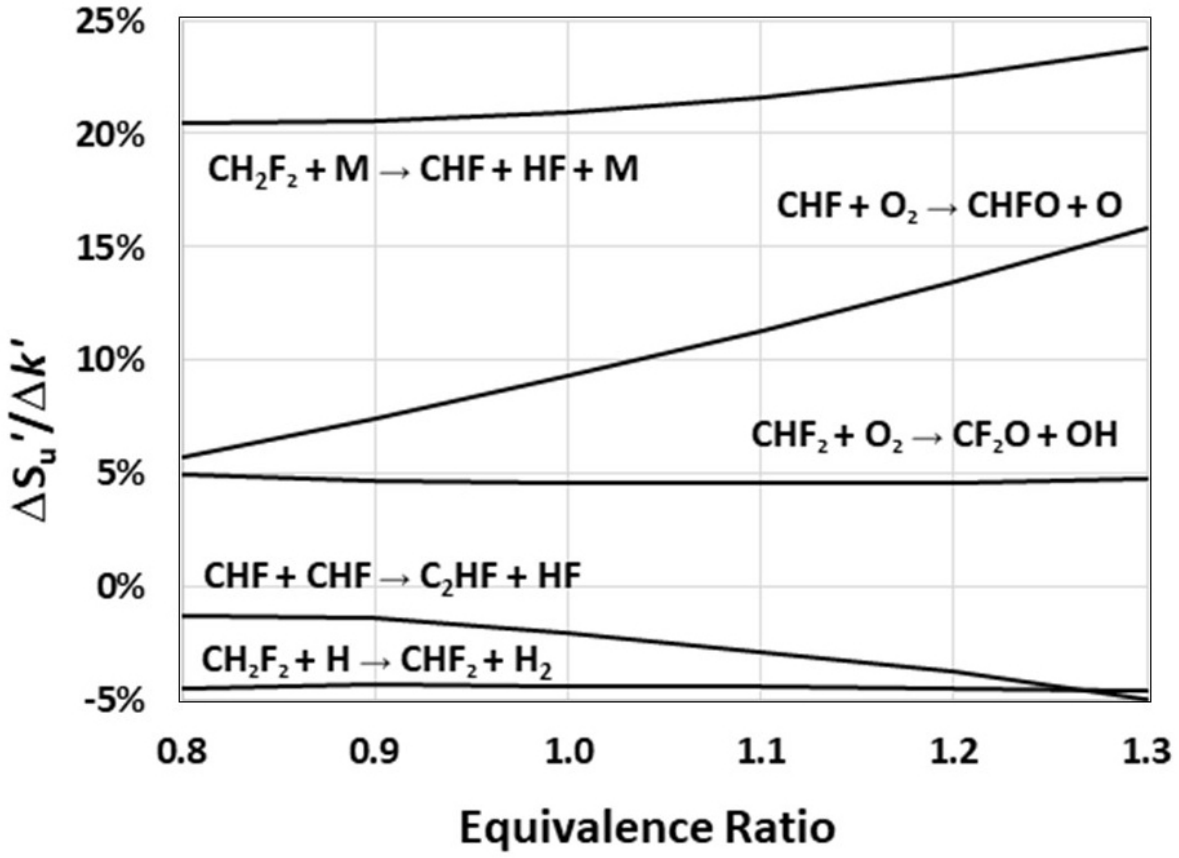

FIGURE 4 Change in burning velocities Su with rate constants k: (Su'/k'), where Su' = Su/Su and k' = k/k. Conditions are 30% O2, P = 2 bar, Tu = 350 K – at other conditions, the dependencies are qualitatively the same, but quantitatively different

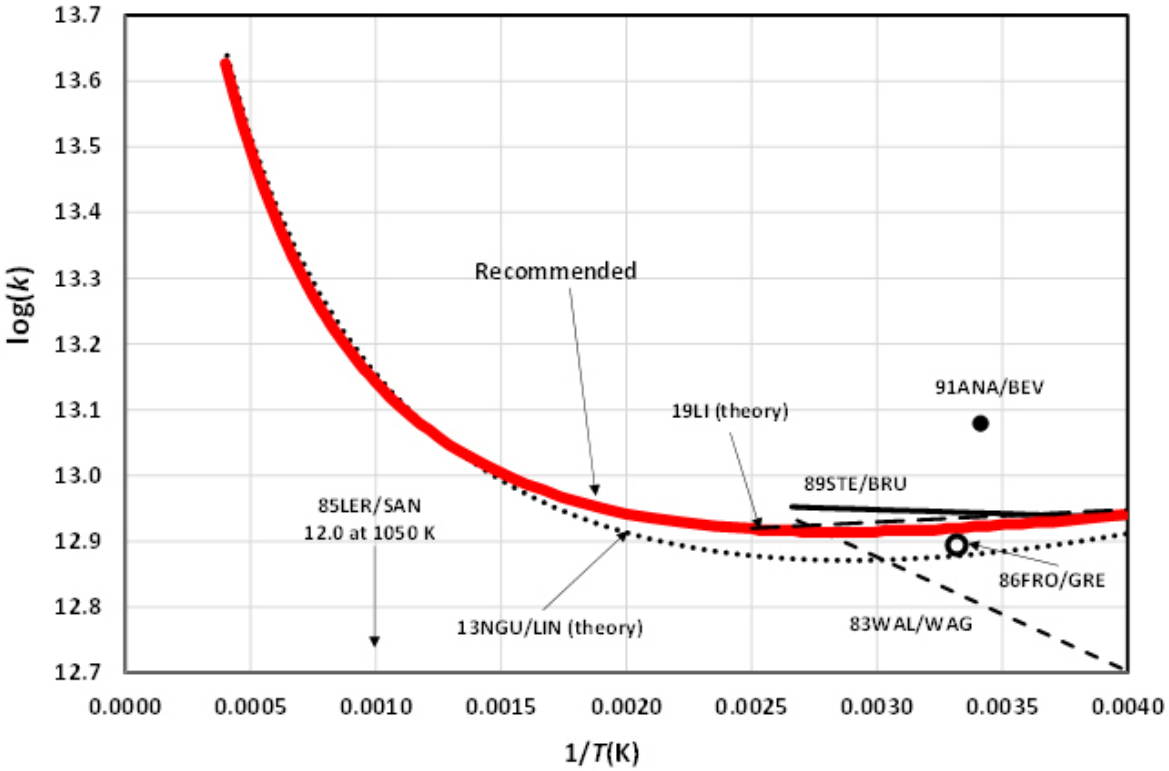

FIGURE 5 Recommended rate expression for H2O + F ⟶ OH + F versus experimental and theoretical values. k (cm3 mol-1 s-1). Recommended (large solid red line), 13NGU/LIN [68] (dotted line), 83WAL/WAG [64] (small dashed line), 85LER/SAN (not shown, off the chart), 86FRO/GRE [66] (unfilled dot), 89STE/BRU [65] (medium solid line), 91ANA/DEV [67] (filled dot), 19LI [70 (large dashed line)

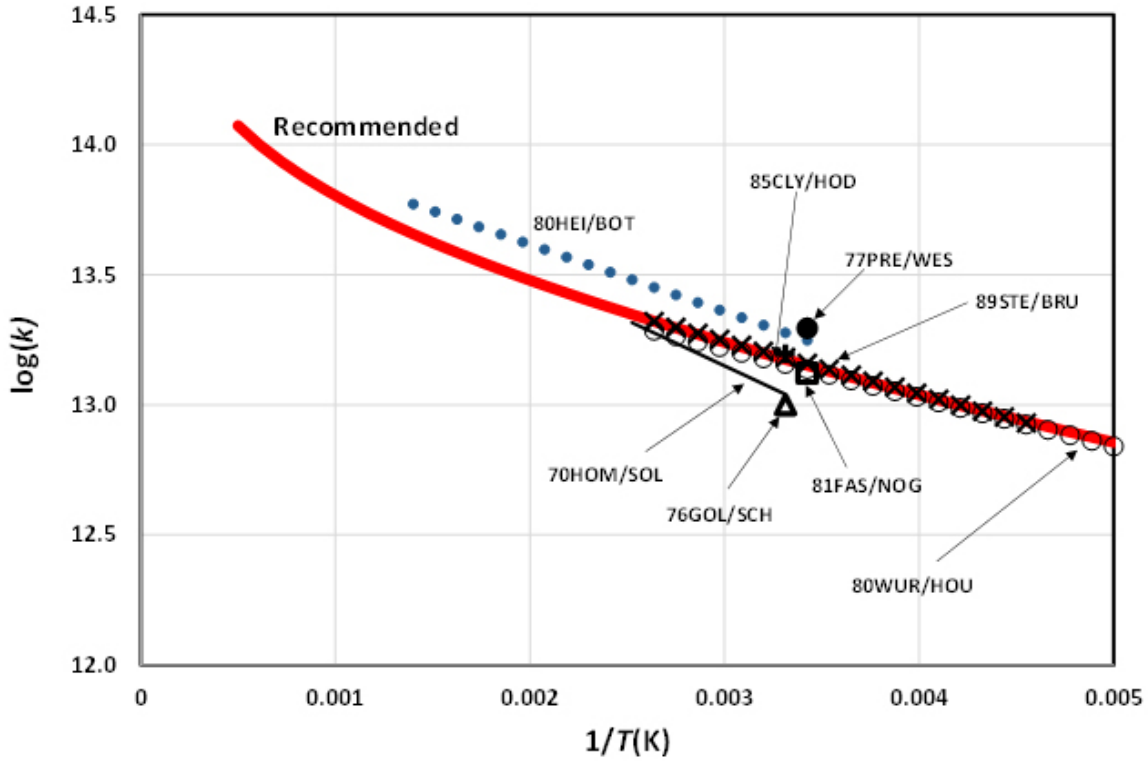

FIGURE 6 Recommended and experimental rate constants for H2 + F ⟶ HF + H. Recommended (thick solid red line), 97PER/KOR(eval) [72] (thick dashed line), 70HOM/SOL [77] (medium solid line), 74IGO/KUL [75] (dashed line), 76GOL/SCH [81] (triangle), 77PRE/WES [79] (large filled dot), 80HEI/ROT [78] (dotted curve), 80WUR/HOU [73] (open circles), 81FAS/NOG [76] (unfilled square), 85CLY/HOD [74] (plus sign), 89STE/BRU [65] (X), 21BED [83] (thin solid line)

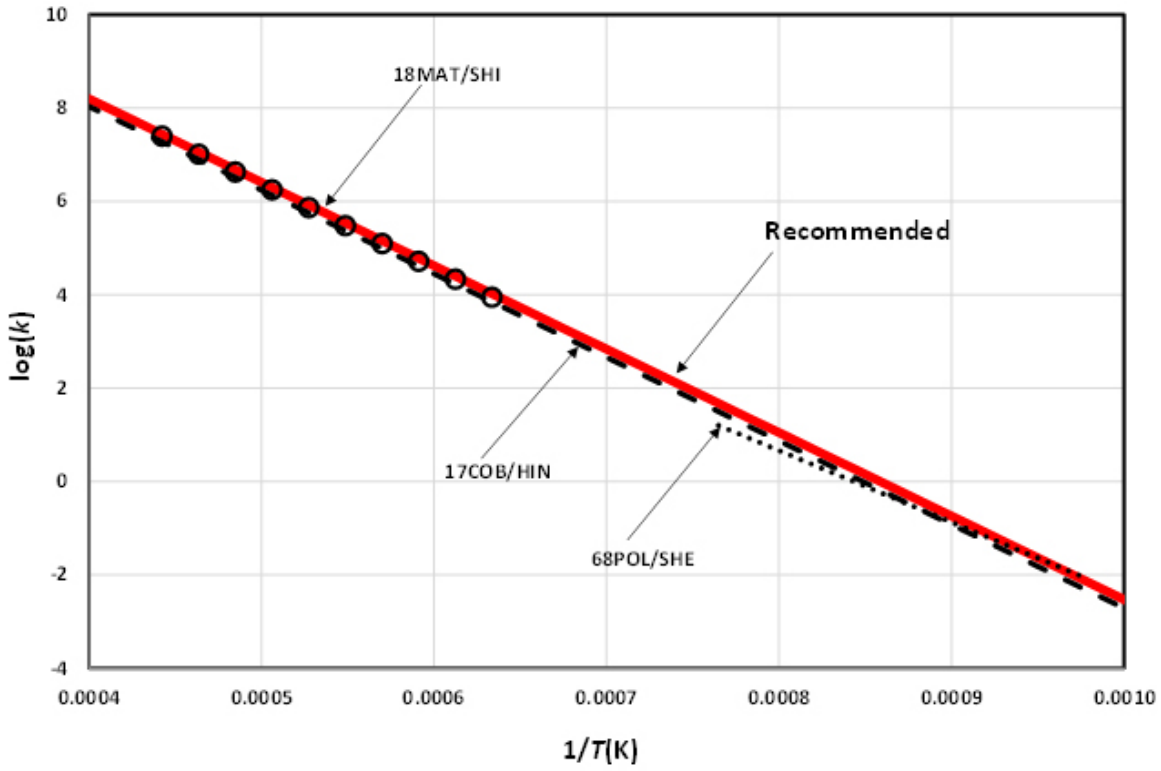

FIGURE 7 CH2F2 → CHF + HF (high pressure limit). Recommended (thick red line), 18MAT/SHI [94] (open circles), 17COB/HIN [93] (dashed line), 68POL/SHE [92] (dotted line)